

Solvent Control in the Protonation of  $[\text{Cp}^*\text{Mo}(\text{dppe})\text{H}_3]$  by  $\text{CF}_3\text{COOH}$ Pavel A. Dub,<sup>[a,b]</sup> Miguel Baya,<sup>[a]</sup> Jennifer Houghton,<sup>[a]</sup> Natalia V. Belkova,<sup>[b]</sup> Jean-Claude Daran,<sup>[a]</sup> Rinaldo Poli,<sup>\*[a]</sup> Lina M. Epstein,<sup>[b]</sup> and Elena S. Shubina<sup>\*[b]</sup>**Keywords:** Molybdenum / Hydrido ligand / Trifluoroacetato ligand / Proton transfer / Dihydrogen bonding

The outcome of the reaction between  $[\text{Cp}^*\text{Mo}(\text{dppe})\text{H}_3]$  [dppe = 1,2-bis(diphenylphosphanyl)ethane] and trifluoroacetic acid (TFA) is highly dependent on the solvent and the TFA/Mo ratio. The dihydride compound  $[\text{Cp}^*\text{Mo}(\text{dppe})\text{H}_2(\text{O}_2\text{CCF}_3)]$  is obtained selectively when the reaction is carried out in aromatic hydrocarbons (benzene, toluene) when using less than one equivalent of TFA. The dihydride is also the end product when THF or MeCN are used as solvent, independent of the TFA/Mo ratio. In benzene/toluene the use of excess acid has a profound effect, resulting in the formation of the tetrahydrido complex  $[\text{Cp}^*\text{Mo}(\text{dppe})\text{H}_4]^+$ , which did not further evolve into the dihydrido product. Monitoring of the reaction by NMR and IR spectroscopy under different conditions (solvent, temperature, TFA/Mo ratio) reveals the rapid establishment of an equilibrium between

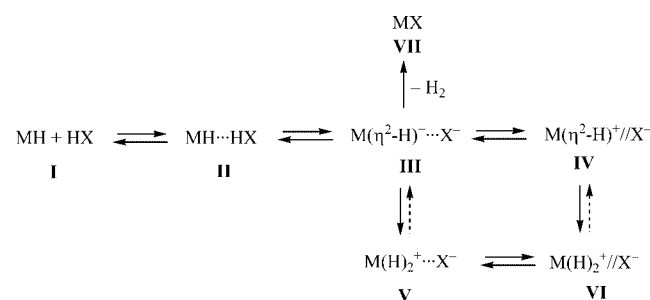
the dihydrogen-bonded adduct,  $[\text{Cp}^*\text{Mo}(\text{dppe})\text{H}_3]\cdots\text{HO}_2\text{CCF}_3$ , the ion-paired proton-transfer product,  $[\text{Cp}^*\text{Mo}(\text{dppe})\text{H}_4]^+\cdots\text{O}_2\text{CCF}_3$ , and the separated ions, followed by a slower irreversible transformation to the final dihydride product with  $\text{H}_2$  evolution. The activation parameters of the  $\text{H}_2$  evolution and M-OR product formation were determined. Excess TFA in low-polarity solvents stabilizes the separated charged species by forming the homoconjugate anion  $[\text{CF}_3\text{COO}(\text{CF}_3\text{COOH})_n]^-$ . The effect of the solvent on the course of the reaction can be interpreted in terms of the different polarity, H-bonding ability, and coordinating power of the various solvent molecules.

(© Wiley-VCH Verlag GmbH & Co. KGaA, 69451 Weinheim, Germany, 2007)

## Introduction

It is now well established that a common proton-transfer pathway from a proton donor HX to a transition-metal hydride complex involves the initial attack of HX on the hydride ligand with formation of a dihydrogen-bonded adduct,  $\text{MH}\cdots\text{HX}$ , followed by proton transfer and production of a nonclassical dihydride (dihydrogen complex) product,  $\text{M}(\eta^2\text{-H}_2)^+$ . The establishment of a hydrogen-bonded ion pair between the nonclassical cation and its counteranion increases the stability of the  $\text{M}(\eta^2\text{-H}_2)^+$  complex and retards its transformation into a classical polyhydride or organyloxo ( $\text{X} = \text{OR}$ ) species (Scheme 1).<sup>[1]</sup>

The formation of  $\text{M}(\eta^2\text{-H}_2)^+\cdots\text{X}^-$  ion pairs (**III**,  $\text{X}^- = \text{CF}_3\text{COO}^-$ ,  $\text{ArO}^-$ ,  $\text{R}^{\text{F}}\text{O}^-$ ), stabilized by hydrogen bonds between the dihydrogen ligand and counteranions, was detected for  $[\text{CpRuH}(\text{CO})(\text{PCy}_3)_3]$ ,<sup>[2,3]</sup>  $\text{PP}_3\text{MH}_2$  { $\text{PP}_3 = \text{P}(\text{CH}_2\text{CH}_2\text{PPh}_2)_3$ },<sup>[4]</sup> and  $[\text{Cp}^*\text{MH}(\text{dppe})]$  ( $\text{M} = \text{Fe}$ ,<sup>[5]</sup>  $\text{Ru}$ )<sup>[6]</sup> complexes by IR and UV/Vis spectroscopy. The ion-



Scheme 1.

pair stability increases with the proton-accepting ability of the anion.<sup>[3]</sup>

Proton transfer may also be assisted by a second molecule of the proton donor HX, depending on the acid strength. In this case, the conjugate base  $\text{X}^-$  in species **III**–**VI** may be present in the form of the homoconjugate anion,  $\text{XHX}^-$ . We have recently shown that the irreversible isomerization of  $[\text{Cp}^*\text{M}(\eta^2\text{-H}_2)(\text{dppe})]^+$  complexes ( $\text{M} = \text{Fe}$ ,<sup>[5]</sup>  $\text{Ru}$ )<sup>[6]</sup> into classical *trans*-dihydride species occurs upon dissociation of the  $\text{M}(\eta^2\text{-H}_2)^+\cdots\text{XHX}^-$  ion pair (i.e., **III** to **IV**). This is indicated by the difference in temperature at which the  $\text{M}(\eta^2\text{-H}_2)^+ \rightarrow \text{M}(\text{H})_2^+$  isomerization process can occur depending on the counteranion; higher temperatures are necessary to induce isomerization in the presence of more basic anions (greater ion-pair stability). Additionally,

[a] Laboratoire de Chimie de Coordination, UPR CNRS 8241 liée par convention à l'Université Paul Sabatier et à l'Institut National Polytechnique de Toulouse, 205 Route de Narbonne, 31077 Toulouse Cedex, France  
Fax: +33-561553003  
E-mail: poli@lcc-toulouse.fr

[b] Nesmeyanov Institute of Organoelement Compounds, Russian Academy of Sciences, Vavilov Street 28, 119991 Moscow, Russia

Supporting information for this article is available on the WWW under <http://www.eurjic.org> or from the author.

the isomerization rate constant does not depend on the anion nature.<sup>[7,8]</sup> In some cases, the nonclassical to classical rearrangement (**III** to **V**, or **IV** to **VI**) is a reversible process.<sup>[9]</sup>

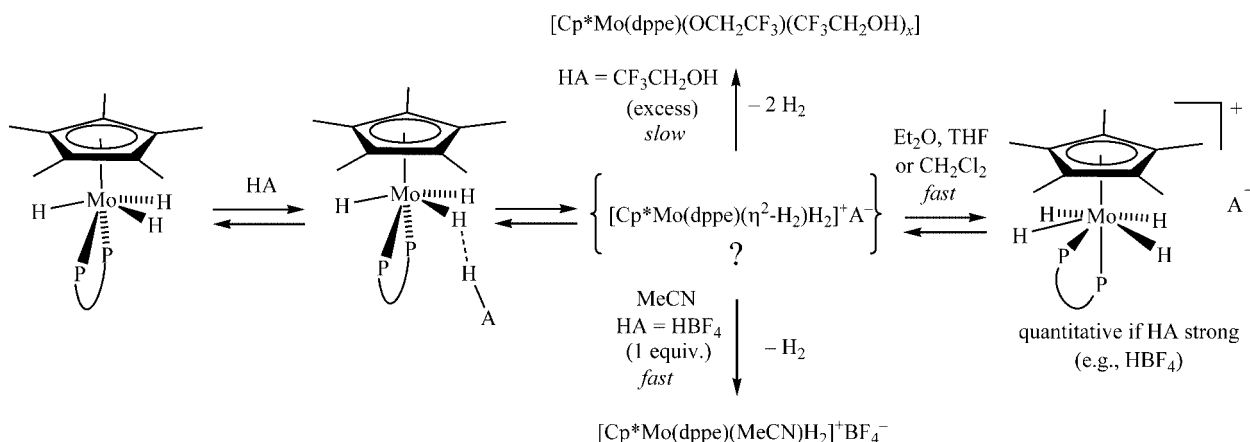
In many cases, however, basic anions ( $X^- = RO^-$ ,  $RCOO^-$ ) tend to displace  $H_2$  from the transition-metal coordination sphere, yielding organyloxo products (i.e., **VII**). This is the case for the protonation of [(triphos)ReH(CO)<sub>2</sub>],<sup>[10]</sup> [Re(CO)H<sub>2</sub>(NO)(PR<sub>3</sub>)<sub>2</sub>],<sup>[11]</sup> and the previously mentioned [CpRuH(CO)(PCy<sub>3</sub>)],<sup>[2]</sup> for which corresponding  $M(\eta^2-H_2)^+X^-$  complexes could be isolated as  $BF_4^-$  salts. These evolved into MX species in the presence of fluorinated alcohols or carboxylic acids. This reaction proceeds intramolecularly without the hydrogen-bonded ion-pair dissociation.<sup>[2]</sup> Most of the M–OR complexes were only characterized in solution; two examples of isolated compounds are [ReH(OC<sub>6</sub>H<sub>4</sub>NO<sub>2</sub>)(CO)(NO)(PMe<sub>3</sub>)<sub>2</sub>]<sup>[11]</sup> and [(triphos)Re(CO)<sub>2</sub>(OCOCH<sub>2</sub>Cl)].<sup>[10]</sup> In addition to the counteranion nature, temperature and solvent polarity could be used to control the stability of the  $M(\eta^2-H_2)^+$  species and the proton-transfer equilibrium position. For example, the substantial increase in the dielectric constant of the Freon mixture (CDCl<sub>2</sub>F/CF<sub>3</sub>, 2:1) at low temperatures was reported to assist the proton transfer to [Cp\**Ru*H<sub>3</sub>(PCy<sub>3</sub>)], yielding [Cp\**Ru*(H)<sub>2</sub>( $\eta^2-H_2$ )(PCy<sub>3</sub>)]<sup>+</sup>OR<sup>-</sup>.<sup>[12]</sup> However, the influence of the medium on the H<sub>2</sub> release process was not studied in detail.

In contrast to all of the described systems, the protonation of the trihydridomolybdenum complex [Cp\*Mo(dppe)H<sub>3</sub>] gave, via the intermediate formation of a dihydrogen-bonded complex, the cationic classical tetrahydride complex [Cp\*Mo(dppe)H<sub>4</sub>]<sup>+</sup> (**V**/**VI**), without the detection of a nonclassical isomer, [Cp\*Mo(dppe)( $\eta^2-H_2$ )-H<sub>2</sub>]<sup>+</sup> (**III**/**IV**). Theoretical calculations, however, located the latter complex on the proton-transfer potential energy surface, with a very low energy barrier for the intramolecular rearrangement.<sup>[13]</sup> Facile access to a nonclassical isomer is evidenced by the evolution of H<sub>2</sub> from [Cp\*Mo(dppe)H<sub>4</sub>]<sup>+</sup> at ambient temperature. We now report new results on the protonation of [Cp\*Mo(dppe)H<sub>3</sub>] using trifluoroacetic acid (TFA) in various solvents of different coordinating (in par-

ticular H-bonding) ability and polarity: benzene, toluene, THF, CH<sub>2</sub>Cl<sub>2</sub>, and MeCN. These reactions led to the formation of a new hydride product with a coordinated trifluoroacetate anion. We will show how subtle changes in the protonation medium may drastically affect the reactivity of [Cp\*Mo(dppe)H<sub>3</sub>] and the stability of its protonation product.

## Results

Since the results of previous investigations into the protonation of [Cp\*Mo(dppe)H<sub>3</sub>]<sup>[13–15]</sup> serve as a basis for the new findings described in this paper, we summarize here the salient points that emerge from those studies. (i) The trihydride complex has a high basicity factor ( $E_j = 1.42 \pm 0.02$ ), placing it in the category of the most hydridic complexes known. (ii) As mentioned in the Introduction, the interaction with HBF<sub>4</sub> in noncoordinating or weakly coordinating solvents (diethyl ether, THF) leads directly to the tetrahydride complex [Cp\*Mo(dppe)H<sub>4</sub>]<sup>+</sup>, without the detection of a nonclassical intermediate, although its presence is suggested by the theoretical calculations. (iii) [Cp\*Mo(dppe)H<sub>4</sub>]<sup>+</sup>BF<sub>4</sub><sup>-</sup> is unstable and rapidly loses dihydrogen; in MeCN, this process leads to the formation of the solvent-stabilized complex [Cp\*Mo(dppe)H<sub>2</sub>(MeCN)]<sup>+</sup>. (iv) The interaction with weaker proton donors [the fluorinated alcohols CH<sub>2</sub>FCH<sub>2</sub>OH, CF<sub>3</sub>CH<sub>2</sub>OH, and (CF<sub>3</sub>)<sub>2</sub>CHOH] in low-polarity solvents (e.g., THF, CH<sub>2</sub>Cl<sub>2</sub>) at low temperatures leads to the observation of intermediate hydrogen-bonded adducts. Infrared spectral analysis, in combination with theoretical calculations, indicates that one of the hydride ligands of [Cp\*Mo(dppe)H<sub>3</sub>] takes part in hydrogen bonding. (v) Proton transfer from the dihydrogen-bonded adduct yields, without the observable intervention of a second HA molecule in the rate-determining step, the tetrahydride product as a 1:1 ion-pair stabilized by a hydrogen bond between the cation and the anion, [Cp\*Mo(dppe)H<sub>4</sub>]<sup>+</sup>⋯A<sup>-</sup>, as established for HA = *p*-nitrophenol and CF<sub>3</sub>CH<sub>2</sub>OH. The proton-transfer reaction is equilibrated for these weaker proton donors. (vi) On a longer timescale,



Scheme 2.

the tetrahydride product  $[\text{Cp}^*\text{Mo}(\text{dppe})\text{H}_4]^+$ , obtained using  $\text{HA} = \text{CF}_3\text{CH}_2\text{OH}$ , evolves at ambient temperature by release of two  $\text{H}_2$  molecules to form the hydride-free product  $[\text{Cp}^*\text{Mo}(\text{dppe})(\text{OCH}_2\text{CF}_3)]$ , probably stabilized by coordination of a second alcohol molecule,  $[\text{Cp}^*\text{Mo}(\text{dppe})(\text{OCH}_2\text{CF}_3)(\text{CF}_3\text{CH}_2\text{OH})]$ . These observations are summarized in Scheme 2.

### Protonation in Benzene/Toluene: Formation of Compound $[\text{Cp}^*\text{Mo}(\text{dppe})\text{H}_2(\text{O}_2\text{CCF}_3)]$

The room-temperature reaction between  $[\text{Cp}^*\text{Mo}(\text{dppe})\text{H}_3]$  and *strictly* 1 equiv. TFA in toluene led selectively to a new dihydride complex,  $[\text{Cp}^*\text{Mo}(\text{dppe})\text{H}_2(\text{O}_2\text{CCF}_3)]$ , as seen in Equation (1). The parallel formation of free  $\text{H}_2$  was confirmed by  $^1\text{H}$  NMR spectroscopic monitoring (characteristic resonance at  $\delta = 4.58$  ppm). The new hydride compound was isolated and fully characterized. It is quite stable in aromatic solvents, decomposing very slowly with generation of free dppe (identified by its  $^{31}\text{P}$  resonance at  $-12.9$  ppm) and other unidentified products that do not contain hydride ligands. Ca. 13% of the product decomposed after 22 hours at room temperature.



The compound is characterized by a hydride resonance centered at  $-5.09$  ppm, with a relative intensity corresponding to two protons, only slightly displaced relative to the hydride resonance of  $[\text{Cp}^*\text{Mo}(\text{dppe})\text{H}_3]$  at  $-5.16$  ppm. The  $^{31}\text{P}\{^1\text{H}\}$  NMR spectrum shows a resonance at 76.9 ppm, which becomes a triplet when selectively decoupled from the dppe proton resonance, confirming the presence of two hydride ligands. The shape of the hydride resonance suggests the occurrence of a dynamic process. A variable-temperature NMR investigation gave further information about this process and also provided longitudinal relaxation times for the hydride resonances. The shape of the  $^1\text{H}$  resonances in the hydride region as a function of temperature is shown in Figure 1 (a). Cooling resulted in broadening and eventual decoalescence (225 K), yielding two broad resonances in a 1:1 ratio at  $-4.19$  and  $-6.24$  ppm. The more upfield resonance starts to resolve into a doublet at the lowest temperature, indicating coupling ( $J \approx 72$  Hz) to another  $I = 1/2$  nucleus, probably one of the two phosphorus donor atoms that therefore appear to be inequivalent. This inequivalence was demonstrated by the variable-temperature  $^{31}\text{P}\{^1\text{H}\}$  NMR investigation (see part b of Figure 1); decoalescence was observed at  $T < 233$  K to yield two resonances in an approximate ratio of 1:1. No P–P coupling can be discerned from the spectra. The  $^{31}\text{P}$  NMR data were used in a lineshape analysis, from which the activation parameters of  $\Delta H^\ddagger = (6.4 \pm 0.4)$  kcal mol $^{-1}$  and  $\Delta S^\ddagger = (10 \pm 2)$  cal K $^{-1}$  mol $^{-1}$  were calculated using an Eyring analysis (see electronic Supporting Information). The lineshape analysis of the  $^1\text{H}$  resonance was complicated by the lack of knowledge of  $J_{\text{HP}}$  data due to broadness in the low-temperature spectra, but

a simulation using the rate constant obtained from the  $^{31}\text{P}$  NMR spectrum and a reasonable guess for the  $J_{\text{HP}}$  values gave a reasonable fit above coalescence, suggesting that the same mechanism is responsible for both H and P exchange processes. A possibility for this mechanism is illustrated in Scheme 3. The  $T_1$  value for the hydride resonance remains rather high throughout the temperature range (see Supporting Information), characteristic of a classical dihydride, with a minimum of 510 ms before decoalescence. For comparison, the  $T_{1\text{min}}$  of complex  $[\text{Cp}^*\text{Mo}(\text{dppe})\text{H}_4]^+$  is 174 ms for the  $\text{BF}_4^-$  salt and 191 ms when obtained by proton transfer from TFE (these measurements were carried out at 400 MHz).<sup>[13]</sup>

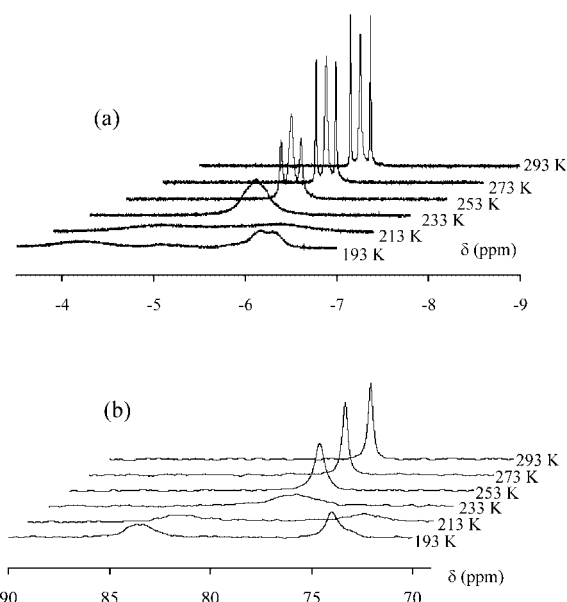
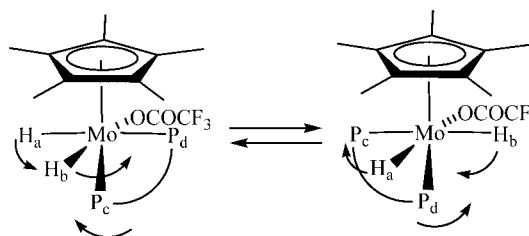


Figure 1. Variable-temperature spectra for compound  $[\text{Cp}^*\text{Mo}(\text{dppe})\text{H}_2(\text{O}_2\text{CCF}_3)]$  in  $\text{C}_6\text{D}_5\text{CD}_3$ : (a)  $^1\text{H}$  NMR (500 MHz); (b)  $^{31}\text{P}\{^1\text{H}\}$  NMR (202 MHz).



Scheme 3.

The chemical composition of the product was confirmed by single-crystal X-ray analysis. The coordination geometry, shown in Figure 2, corresponds to a rather severely distorted octahedron if the  $\text{Cp}^*$  ligand is considered to occupy a single coordination position at the ring centroid. This distortion is caused by steric repulsion between the  $\text{Cp}^*$  and dppe ligands and by the small size of the two hydride ligands, which force the pseudoaxial (*trans* to the  $\text{Cp}^*$  ligand) phosphorus donor to move up into the wedge of the two Mo–H bonds. The  $\text{CNT-Mo1-P1}$  angle [ $122.648(13)^\circ$ ] is greater than the  $\text{CNT-Mo1-O1}$ ,  $\text{CNT-Mo1-H1}$ , and

CNT–Mo1–H2 angles [119.74(4)°, 98.5(10)°, and 96.9(9)°, respectively], whereas the CNT–Mo1–P2 angle [144.369(14)°] is much smaller than 180°. A similar distortion was observed in the structure of the related [Cp\*Mo(dppe)H(MeCN)<sub>2</sub>]<sup>2+</sup> complex.<sup>[14]</sup> The other notable feature is the monodentate coordination of the trifluoroacetate ligand, which occupies a pseudoequatorial position *cis* to the P1 and H1 donors and *trans* to H2. The Mo1–O1 bond length [2.2008(15) Å] is unexpectedly longer than those found in other Mo monodentate carboxylate derivatives in the same or lower oxidation state, for example, 2.167(4) Å found in [Cp\*Mo<sup>II</sup>(CO)(PMe<sub>3</sub>)<sub>2</sub>(O<sub>2</sub>CMe)],<sup>[16]</sup> 2.102(3) and 2.092(3) Å found in [CpMo<sup>III</sup>(η<sup>4</sup>-C<sub>4</sub>H<sub>6</sub>)(O<sub>2</sub>CCF<sub>3</sub>)<sub>2</sub>],<sup>[17]</sup> and 2.113(4) and 2.102(4) Å found in [Cp<sub>2</sub>Mo<sup>IV</sup>(O<sub>2</sub>CPh)<sub>2</sub>].<sup>[18]</sup> Another interesting feature is the similar C8–O1 [1.249(3) Å] and C8–O2 [1.221(3) Å] distances (bond difference Δ = 0.028 Å). These are not quite as long or short, respectively, as expected for localized single and double bonds. For instance, the recently determined structure of Ph<sub>3</sub>CCH<sub>2</sub>COOH shows clearly defined C–O [1.304(3) Å] and C=O [1.203(3) Å] bonds (Δ = 0.101 Å) with no obvious sign of hydrogen atom disorder.<sup>[19]</sup> The monodentate carboxylate C–O distances in the mentioned examples show larger differences between C=O and C–O bond lengths, although not quite as large as those found in free carboxylic acids, namely 1.277(8) Å compared with 1.212(8) Å (Δ = 0.065 Å) for [Cp\*Mo<sup>II</sup>(CO)(PMe<sub>3</sub>)<sub>2</sub>(O<sub>2</sub>CMe)],<sup>[16]</sup> 1.276(5) and 1.255(5) Å compared with 1.200(5) and 1.192(6) Å (Δ = 0.076 and 0.063 Å, respectively) for [CpMo<sup>III</sup>(η<sup>4</sup>-C<sub>4</sub>H<sub>6</sub>)(O<sub>2</sub>CCF<sub>3</sub>)<sub>2</sub>],<sup>[17]</sup> and 1.281(8) and 1.300(8) Å compared with 1.208(8) and 1.210(8) Å (Δ = 0.073 and 0.090 Å, respectively) for [Cp<sub>2</sub>Mo<sup>IV</sup>(O<sub>2</sub>-CPh)<sub>2</sub>].<sup>[18]</sup> This combined evidence indicates a significant ionic contribution to the bond between the Mo center and the monodentate anion, which then continues to promote some electronic delocalization between the two C–O bonds. Other relevant structural parameters are listed in Table 1.

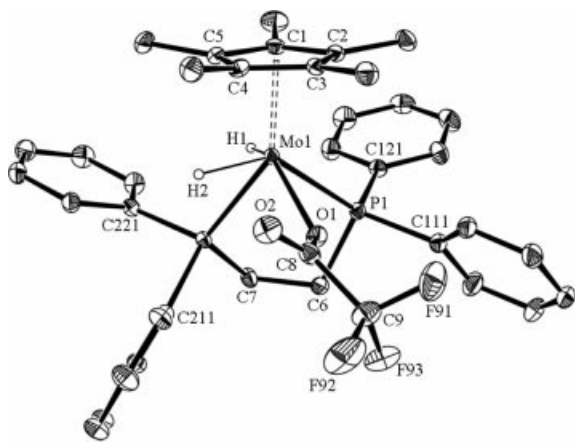


Figure 2. ORTEP view of compound [Cp\*Mo(dppe)H<sub>2</sub>(OCOCF<sub>3</sub>)]. Hydrogen atoms, except for the two hydride ligands, are omitted for clarity. The thermal ellipsoids are drawn at the 30% probability level.

Table 1. Selected bond lengths [Å] and angles [°] for compound [Cp\*Mo(dppe)H<sub>2</sub>(OCOCF<sub>3</sub>)].

Mo1–CNT	1.96462(17)	Mo1–O1	2.2008(15)
Mo1–P1	2.5206(5)	Mo1–P2	2.3962(5)
Mo1–H1	1.60(3)	Mo1–H2	1.65(3)
P1–C111	1.833(2)	P2–C211	1.8459(19)
P1–C121	1.834(2)	P2–C221	1.828(2)
P1–C6	1.844(2)	P2–C7	1.849(2)
C6–C7	1.526(3)	C8–C9	1.547(3)
C8–O1	1.249(3)	C8–O2	1.221(3)
CNT–Mo1–O1	119.74(4)		
P2–Mo1–P1	81.360(17)	H2–Mo1–H1	105.6(14)
CNT–Mo1–P1	122.648(13)	CNT–Mo1–P2	144.369(14)
O1–Mo1–P1	76.82(4)	O1–Mo1–P2	89.40(4)
CNT–Mo1–H1	98.5(10)	CNT–Mo1–H2	96.9(9)
O1–Mo1–H1	139.8(10)	O1–Mo1–H2	83.0(10)
P2–Mo1–H1	61.6(10)	P2–Mo1–H2	64.6(9)
P1–Mo1–H1	72.0(11)	P1–Mo1–H2	140.5(9)

Compound [Cp\*Mo(dppe)H<sub>2</sub>(OCOCF<sub>3</sub>)] exhibits two intense overlapping ν<sup>as</sup><sub>OCO</sub> bands in the IR spectrum; the frequencies and relative intensities of which are solvent dependent (see Table 2). As the solvent polarity increases, A<sub>low</sub>/A<sub>high</sub> decreases and Δν = (ν<sub>high</sub> – ν<sub>low</sub>) increases. The same behavior was observed previously for [CpM(CO)<sub>2</sub>(OCOR)] complexes (M = Fe, Ru)<sup>[20]</sup> and was explained by the presence of a Fermi resonance between the fundamental ν<sup>as</sup><sub>OCO</sub> stretching vibration and an overtone or combination band of very close frequency. The larger intensity ratio observed in CH<sub>2</sub>Cl<sub>2</sub> could be explained by the different nature of the solute–solvent interaction, since this solvent could act as a proton donor and form hydrogen bonds with the carboxyl group coordinated to the metal.

Table 2. Characteristics of the ν<sup>as</sup><sub>OCO</sub> band of [Cp\*Mo(dppe)H<sub>2</sub>(OCOCF<sub>3</sub>)] in the solid state and in solution.

Solvent	ν <sup>as</sup> <sub>OCO</sub> /cm <sup>-1</sup>	Δν	Intensity ratio (A <sub>low</sub> /A <sub>high</sub> )
Solid (KBr)	1700 sh, 1685 s	15	1.8
C <sub>6</sub> H <sub>6</sub>	1700 sh, 1690	10	1.2
C <sub>6</sub> D <sub>5</sub> CD <sub>3</sub>	1700 sh, 1690	10	1.1
THF	1702, 1690	12	1.0
CH <sub>2</sub> Cl <sub>2</sub>	1706 sh, 1688	18	2.2

### Protonation in Benzene/Toluene: Evolution with Time

The <sup>1</sup>H NMR spectroscopic monitoring of the [Cp\*Mo(dppe)H<sub>3</sub>]-TFA reaction in C<sub>6</sub>D<sub>6</sub> at different TFA/Mo ratios at room temperature was most enlightening. Figure 3 (a) shows the spectrum of the starting material before TFA addition.<sup>[21]</sup>

When using a 10-fold excess of TFA, the tetrahydrido complex [Cp\*Mo(dppe)H<sub>4</sub>]<sup>+</sup> was the only observed product, see Figure 3 (b). This is characterized by a hydride triplet resonance at –3.57 ppm (J<sub>HP</sub> = 37.9 Hz) in the <sup>1</sup>H NMR spectrum and by a <sup>31</sup>P resonance at 72.3 ppm in C<sub>6</sub>D<sub>6</sub>, quite close to the values previously reported for the BF<sub>4</sub><sup>–</sup> salt in CDFCl<sub>2</sub> at –60 °C.<sup>[14]</sup> In agreement with the literature, decomposition takes place at room temperature (90% after

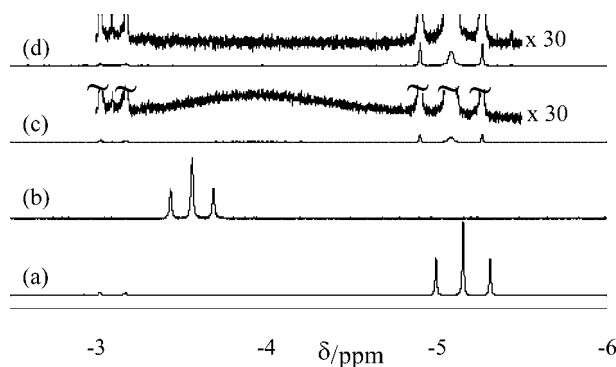


Figure 3.  $^1\text{H}$  NMR (300 MHz) spectroscopic monitoring of the reaction between  $[\text{Cp}^*\text{Mo}(\text{dppe})\text{H}_3]$  and TFA in  $\text{C}_6\text{D}_6$  (290 K): (a) starting material before the TFA addition; (b) immediately after the TFA addition (10 equiv.); (c) immediately after the TFA addition (1 equiv.); (d) after 3.5 h from spectrum (c).

ca. 25 minutes), without yielding any hydride-containing product. This decomposition was not investigated in any further detail.

For the 1:1 reaction, a broad resonance was initially present in the hydride region at an intermediate position between those of the trihydride and tetrahydride complexes, in addition to the final product resonance (Figure 3, c). The position and shape of the broad resonance depends on the TFA/Mo ratio and on the temperature (vide infra). The  $^{31}\text{P}\{^1\text{H}\}$  NMR spectrum at room temperature exhibits two small and broadened resonances at the characteristic positions of the trihydride complex ( $\delta = 91.4$  ppm) and the tetrahydride protonation product ( $\delta = 72.3$  ppm),<sup>[22]</sup> in addition to the sharp resonance of the  $[\text{Cp}^*\text{Mo}(\text{dppe})\text{H}_2(\text{O}_2\text{CCF}_3)]$  product at 76.9 ppm and a minor contaminant resonance.<sup>[21]</sup> This suggests that the broad  $^1\text{H}$  resonance results from a rapid degenerate exchange between the starting complex  $[\text{Cp}^*\text{Mo}(\text{dppe})\text{H}_3]$ , which is not completely consumed, and its protonation product,  $[\text{Cp}^*\text{Mo}(\text{dppe})\text{H}_4]^+$ . This exchange will be addressed in further detail in the next section. Given the larger chemical shift difference between the  $^{31}\text{P}$  resonances, the shape of the  $^{31}\text{P}$  NMR spectrum is much closer to the slow exchange limit than that of the  $^1\text{H}$  NMR spectrum. After a few hours at room temperature (or upon brief warming to ca. 40 °C), the broad band disappears and the resonance corresponding to  $[\text{Cp}^*\text{Mo}(\text{dppe})\text{H}_2(\text{OCOCF}_3)]$  increases in intensity (Figure 3, d). These observations reveal the presence of an equilibrium between the tetrahydride complex and the starting trihydride complex, followed by a slow irreversible conversion to the final product by  $\text{H}_2$  loss.

A variable-temperature study of the reaction mixture in  $\text{C}_6\text{D}_5\text{CD}_3$ , carried out immediately after mixing the reagents in a 1:1 ratio, confirmed the earlier assignments. The hydride resonance of the dihydride product evolved as discussed previously (Figure 1, a), whereas the broad resonance at  $-3.63$  ppm decoalesced at  $T < 270$  K to yield two resonances at the expected positions of  $[\text{Cp}^*\text{Mo}(\text{dppe})\text{H}_3]$  and  $[\text{Cp}^*\text{Mo}(\text{dppe})\text{H}_4]^+$ . The incomplete protonation in the presence of a stoichiometric amount of TFA shows that the

protonation process is at equilibrium using this particular proton donor. Both complexes exhibit sharp resonances when alone and also when mixed together with  $[\text{Cp}^*\text{Mo}(\text{dppe})\text{H}_2(\text{OCOCF}_3)]$ . Interestingly, the hydride resonance of  $[\text{Cp}^*\text{Mo}(\text{dppe})\text{H}_4]^+$  broadens again at  $T < 240$  K, but does not decoalesce. On the other hand, the  $\text{BF}_4^-$  salt of this complex was previously reported to retain sharp lines in the  $^1\text{H}$ - and  $^{31}\text{P}$  NMR spectra down to  $-90$  °C, indicating rapid equilibration between the inequivalent H sites.<sup>[14]</sup> This suggests that the hydride scrambling process is slowed down by hydrogen bonding between  $[\text{Cp}^*\text{Mo}(\text{dppe})\text{H}_4]^+$  and  $\text{CF}_3\text{COO}^-$ .

The reaction with 3 equiv. TFA resulted in the observation of a sharp resonance at the chemical shift of the tetrahydride complex (indicating essentially complete disappearance of the starting trihydride reagent) and no significant amount of the dihydride product. The subsequent addition of 2 equiv.  $\text{Et}_2\text{NH}$  to this solution led to the formation of complex  $[\text{Cp}^*\text{Mo}(\text{dppe})\text{H}_2(\text{OCOCF}_3)]$  cleanly and quantitatively. When using 1.5 equiv. TFA, rather sharp resonances for the tetrahydride complex and the final dihydride product were initially observed by  $^1\text{H}$  NMR spectroscopic monitoring, but the latter was once again the only observable species remaining at the end of the reaction (ca. 30 minutes at 290 K). When using only 0.5 equiv. TFA, on the other hand, a broad resonance was again initially present, but its chemical shift was closer to that of the starting hydride complex (see Figure 4). This is as expected because the equilibrium mixture of the rapidly exchanging  $[\text{Cp}^*\text{Mo}(\text{dppe})\text{H}_3]$  and  $[\text{Cp}^*\text{Mo}(\text{dppe})\text{H}_4]^+$  complexes is now richer in the former. The formation of the final dihydride product was slower (equilibrium was attained in ca. two hours at 290 K), and ca. 50% of the initial trihydride remained unreacted. As  $[\text{Cp}^*\text{Mo}(\text{dppe})\text{H}_4]^+$  reacted to yield  $[\text{Cp}^*\text{Mo}(\text{dppe})\text{H}_2(\text{OCOCF}_3)]$ , the resonance corresponding to  $[\text{Cp}^*\text{Mo}(\text{dppe})\text{H}_3]$  sharpened. The addition of excess TFA to a solution containing  $[\text{Cp}^*\text{Mo}(\text{dppe})\text{H}_2(\text{OCOCF}_3)]$  did not lead to any reaction, in particular no tetrahydride resonance was observed under these conditions.

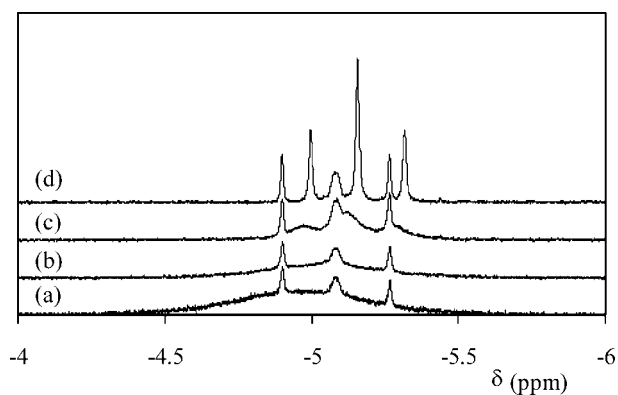


Figure 4.  $^1\text{H}$  NMR (300 MHz) spectroscopic monitoring of the reaction between  $[\text{Cp}^*\text{Mo}(\text{dppe})\text{H}_3]$  and TFA (1:0.5 ratio) in  $\text{C}_6\text{D}_6$  (290 K): (a) recorded immediately; (b) after 7 min; (c) 28 min; (d) 155 min.

We also investigated the reaction between  $[\text{Cp}^*\text{Mo}(\text{dppe})\text{H}_3]$  and  $\text{CF}_3\text{COOD}$  (1 equiv.) by  $^1\text{H}$  NMR spectroscopy in  $\text{C}_6\text{D}_5\text{CD}_3$ . The reaction progressed in an essentially identical manner to that when  $\text{CF}_3\text{COOH}$  was used: immediate observation of the virtual triplet at  $-5.25$  ppm due to the final product and a broad resonance centered at ca.  $-3.6$  ppm. The latter disappears upon brief warming to ca.  $40^\circ\text{C}$ . However, the NMR spectrum shows the formation of  $\text{H}_2$  and  $\text{HD}$  in ca. 3:1 ratio. This is not surprising since all hydride positions in the tetrahydride complex are readily scrambled, therefore the elimination of  $\text{H}_2$  from the  $[\text{Cp}^*\text{Mo}(\text{dppe})\text{H}_3\text{D}]^+$  cation will be statistically favored. The molybdenum product resulting from this reaction should therefore contain both H and D. The hydride resonance does not show evidence for the presence of isotopomers, probably because the isotope shift is too small. The formation of deuterated product(s),  $[\text{Cp}^*\text{Mo}(\text{dppe})\text{HD}(\text{O}_2\text{CCF}_3)]$  and/or  $[\text{Cp}^*\text{Mo}(\text{dppe})\text{D}_2(\text{O}_2\text{CCF}_3)]$ , however, was confirmed by a  $^2\text{H}$  NMR-spectroscopic study, which revealed a binomial triplet resonance at  $-5.9$  ppm with  $J_{\text{PD}} = 7.7$  Hz.

#### Protonation in Other Solvents: NMR-Spectroscopic Study

The solvent has a significant effect on the course of the protonation reaction. The behavior in  $[\text{D}_8]\text{thf}$  is similar but not identical to that in aromatic hydrocarbons (see Figure 5); use of a (sub)stoichiometric amount of the acid initially yields a broad hydride resonance (Figure 5, b). Time evolution at these ratios leads to sharpening of the signals as the irreversible  $\text{H}_2$  elimination and  $[\text{Cp}^*\text{Mo}(\text{dppe})\text{H}_2(\text{O}_2\text{CCF}_3)]$  formation takes place: a similar process to that shown in Figure 4 for the benzene solution. When the sample corresponding to Figure 5 (b) was treated with additional TFA (total 1.5 equiv.), quantitative formation of the dihydride product occurred (Figure 5, c). Use of a large excess (10 equiv.) of  $\text{CF}_3\text{COOH}$  affords a sharp triplet corresponding to the tetrahydrido cation and a strong resonance for the  $[\text{Cp}^*\text{Mo}(\text{dppe})\text{H}_2(\text{O}_2\text{CCF}_3)]$  product (Figure 5, d). As in  $\text{C}_6\text{D}_6$  or  $\text{C}_6\text{D}_5\text{CD}_3$ , a broad resonance is not obtained at this ratio. However, with time, the tetrahydride resonance disappears and the dihydride resonance increases in  $[\text{D}_8]\text{thf}$  (Figure 5, e), whereas in the analogous benzene solution decomposition occurs without formation of the dihydride product, as stated earlier.

THF was found to be a suitable solvent in which to probe the nature of the degenerate exchange between  $[\text{Cp}^*\text{Mo}(\text{dppe})\text{H}_3]$  and  $[\text{Cp}^*\text{Mo}(\text{dppe})\text{H}_4]^+$ , by repeating the protonation in the presence of  $\text{HBF}_4$  instead of  $\text{CF}_3\text{COOH}$  (the  $\text{BF}_4^-$  salt of the tetrahydride product is soluble in THF, but precipitates from toluene or benzene). If the exchange takes place bimolecularly via a symmetrical  $[\text{Cp}^*(\text{dppe})\text{H}_3\text{Mo}\cdots\text{H}\cdots\text{MoH}_3(\text{dppe})\text{Cp}^*]^+$  transition state, the line-shape of the signal will not depend on the nature of the acid. On the other hand, a unimolecular pathway involving the conjugate base of the proton donor should yield a slower exchange rate for the  $\text{BF}_4^-$  sample, because this is a much weaker base than  $\text{CF}_3\text{COO}^-$ . The NMR-spectroscopic

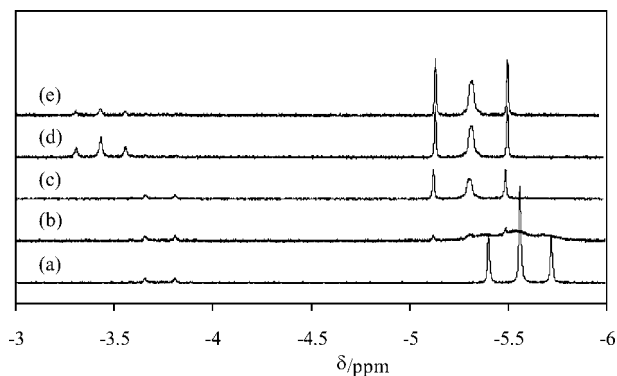


Figure 5.  $^1\text{H}$  NMR (300 MHz) spectroscopic monitoring of the reaction between  $[\text{Cp}^*\text{Mo}(\text{dppe})\text{H}_3]$  and TFA in  $[\text{D}_8]\text{thf}$  (290 K): (a) before the TFA addition; (b) TFA/Mo = 0.5, 8 min; (c) further addition of 1 equiv. to sample (b): TFA/Mo = 1.5, 30 min; (d) TFA/Mo = 10, immediately after the addition; (e) after 13 min from spectrum (d). The doublet resonance at  $\delta = -3.73$  ppm belongs to the  $[\text{Cp}^*\text{Mo}(\kappa^1\text{-dppe})\text{H}_3]$  contaminant.<sup>[14]</sup>

study of a 2:1  $[\text{Cp}^*\text{Mo}(\text{dppe})\text{H}_3]/\text{HBF}_4$  mixture provides evidence in favor of the unimolecular pathway. As seen in Figure 6, addition of 0.5 equiv.  $\text{HBF}_4$  results in a decrease in the  $[\text{Cp}^*\text{Mo}(\text{dppe})\text{H}_3]$  resonance and the appearance of the  $[\text{Cp}^*\text{Mo}(\text{dppe})\text{H}_4]^+$  resonance, plus a weak triplet resonance at  $-5.65$  ppm ( $J_{\text{HP}} = 53.5$  Hz), whilst the doublet resonance of the  $[\text{Cp}^*\text{Mo}(\kappa^1\text{-dppe})\text{H}_3]$  contaminant remains unchanged. The trihydride and tetrahydride complexes give separated sharp resonances, contrary to the same situation in the presence of trifluoroacetate anion in the same solvent (Figure 5, b). This clearly demonstrates that the anion determines the rate of degenerate exchange. This exchange process therefore involves the hydrogen-bonded ion pair  $[\text{Cp}^*\text{Mo}(\text{dppe})\text{H}_4]^+\cdots\text{O}_2\text{CCF}_3$  and the dihydrogen-bonded trihydride  $[\text{Cp}^*\text{Mo}(\text{dppe})\text{H}_3]\cdots\text{HO}_2\text{CCF}_3$ , the latter being in further rapid equilibration with free trihydride and TFA. Analogous broadening phenomena for hydride signals as a consequence of dihydrogen bonding and equilibrated proton transfer were noted previously in other cases, although the broadening effect was limited to a few Hz in most cases.<sup>[2,23]</sup>

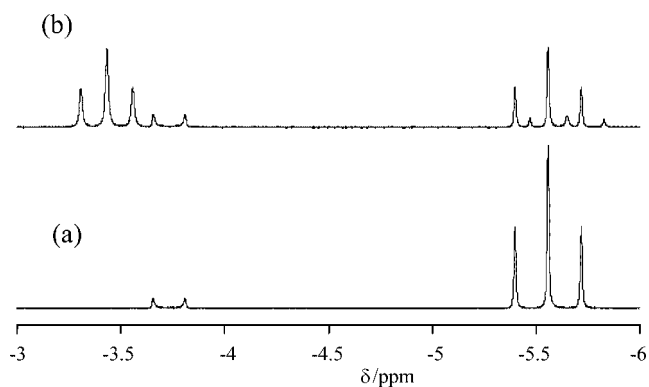


Figure 6.  $^1\text{H}$  NMR-spectroscopic study of a  $[\text{Cp}^*\text{Mo}(\text{dppe})\text{H}_3]/\text{HBF}_4$  mixture in  $[\text{D}_8]\text{thf}$ : (a) starting compound; (b) 21 min after the addition of 0.5 equiv.  $\text{HBF}_4$ . The doublet resonance at  $\delta = -3.73$  ppm belongs to the  $[\text{Cp}^*\text{Mo}(\kappa^1\text{-dppe})\text{H}_3]$  contaminant.<sup>[14]</sup>

The new triplet resonance at  $-5.65$  ppm in Figure 6 is assigned to complex  $[\text{Cp}^*\text{Mo}(\text{dppe})\text{H}_2(\text{THF})]^+$ . It is associated with a new  $^{31}\text{P}\{^1\text{H}\}$  resonance at  $70.7$  ppm. For comparison, the related  $[\text{Cp}^*\text{Mo}(\text{dppe})\text{H}_2(\text{MeCN})]^+$  complex, obtained from the protonation of  $[\text{Cp}^*\text{Mo}(\text{dppe})\text{H}_3]$  by  $\text{HBF}_4$  in  $\text{MeCN}$ ,<sup>[14]</sup> displays a proton resonance at  $-5.50$  ppm ( $J_{\text{P1}} = 51$  Hz,  $J_{\text{P2}} = 52$  Hz) and a phosphorus resonance at  $78.1$  ppm. NMR spectroscopic monitoring shows that this resonance grows while the resonance of the tetrahydride product simultaneously decreases. Interesting features to note are (i) this cationic THF adduct is not observed in the protonation experiment with  $\text{CF}_3\text{COOH}$ ; (ii) the rate of disappearance of the tetrahydride complex is much slower in the presence of the  $\text{BF}_4^-$  anion than in the presence of the  $\text{CF}_3\text{COO}^-$  anion (cf. Figure 6 with Figure 5); and (iii) conversion to the THF solvent adduct appears to be much slower than the analogous reaction in  $\text{MeCN}$ , which was reported to lead to vigorous gas evolution and quantitative production of the  $\text{MeCN}$  complex within 60 minutes.<sup>[14]</sup>

When using  $\text{CH}_2\text{Cl}_2$  as the solvent, the initially formed tetrahydride complex displayed a sharper resonance, even when as little as 0.5 equiv. of the acid was used. The formation of minor amounts of  $[\text{Cp}^*\text{Mo}(\text{dppe})\text{H}_2(\text{O}_2\text{CCF}_3)]$  was also detected (ca. 10% for the 1 equiv. experiment). In this solvent, however, the interpretation of the data is difficult because of the instability of the starting material, the cationic tetrahydride intermediate, and the product (24% decomposition within one hour at room temperature).

Finally, the results of the protonation with TFA (0.5 and 1 equiv.) in  $[\text{D}_3]\text{MeCN}$  at room temperature are shown in Figure 7. In both cases, the immediate formation of  $[\text{Cp}^*\text{Mo}(\text{dppe})\text{H}_2(\text{O}_2\text{CCF}_3)]$  and  $[\text{Cp}^*\text{Mo}(\text{dppe})\text{H}_4]^+$  was observed. When using 0.5 equiv., the resonances corresponding to the tetrahydride complex and trihydride residual starting compound are separate and relatively sharp (see Figure 7, a): a similar situation to that seen in  $\text{CD}_2\text{Cl}_2$  using TFA as the proton donor or in  $[\text{D}_8]\text{thf}$  using  $\text{HBF}_4$ . This indicates that the degenerate exchange is slow under these conditions contrary to the situations in  $[\text{D}_8]\text{thf}$  and  $\text{C}_6\text{D}_6$  using TFA as the proton donor. In turn, this suggests that weak ion pairing occurs, if any, between the tetrahydrido cation and the trifluoroacetate anion in  $[\text{D}_3]\text{MeCN}$ . The conversion of the tetrahydride complex to  $[\text{Cp}^*\text{Mo}(\text{dppe})\text{H}_2(\text{O}_2\text{CCF}_3)]$  was relatively fast and quantitative, see parts b–d in Figure 7. As already noted, when the reaction was carried out in THF the final product was the trifluoroacetate compound rather than the solvent adduct  $[\text{Cp}^*\text{Mo}(\text{dppe})\text{H}_2(\text{MeCN})]^+$  (previously shown to result from the interaction with  $\text{HBF}_4$ ), implying that the ligand exchange shown in Equation (2) ( $\text{S} = \text{THF}, \text{MeCN}$ ) is completely displaced towards the right.

A first comparison of the behavior of  $[\text{Cp}^*\text{Mo}(\text{dppe})\text{H}_4]^+$  in noncoordinating solvents confirms the complex instability, as previously shown for the  $\text{BF}_4^-$  salt, leading to hydride-free decomposition products.<sup>[14]</sup> However, in the presence of either coordinating solvents or the  $\text{CF}_3\text{COO}^-$  anion, efficient trapping of the 16-electron product of  $\text{H}_2$

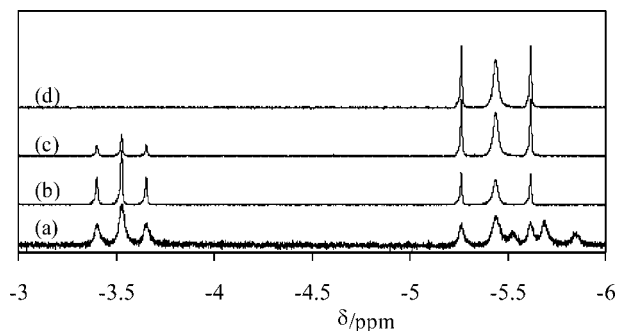


Figure 7.  $^1\text{H}$  NMR-spectroscopic study of the  $[\text{Cp}^*\text{Mo}(\text{dppe})\text{H}_3]^+$ –TFA reaction in  $[\text{D}_3]\text{MeCN}$  at room temperature: (a) 0.5 equiv. TFA, recorded immediately; (b) 1 equiv. TFA, recorded immediately; (c) after 9 min from spectrum (b); (d) 40 min after spectrum (b).



dissociation,  $[\text{Cp}^*\text{Mo}(\text{dppe})\text{H}_2]^+$ , is achieved. The coordinating  $\text{CF}_3\text{COO}^-$  anion is an even better trap than THF and  $\text{MeCN}$ . The nature of the solvent has a dramatic effect on two related features: (i) the ability of the  $\text{CF}_3\text{COO}^-$  anion to attack the cationic complex and yield the neutral dihydride-trifluoroacetate product and (ii) the rate of degenerate exchange between  $[\text{Cp}^*\text{Mo}(\text{dppe})\text{H}_3]$  and  $[\text{Cp}^*\text{Mo}(\text{dppe})\text{H}_4]^+$ . The way in which these two processes are affected by the solvent properties will be addressed in more detail in a later section.

## IR Studies

As equilibrium positions and reaction rates are expected to strongly depend on the solvent's ability to influence hydrogen bonding and ion pairing equilibria, we considered that additional useful information could be gathered from infrared investigations, especially at low temperature where ion pairing and hydrogen bonding are favored. The dielectric permittivity,  $\epsilon$ , increases at ambient temperature in the order toluene (2.4) < THF (7.8) <  $\text{CH}_2\text{Cl}_2$  (8.3) <<  $\text{MeCN}$  (35.9).<sup>[24]</sup> It increases substantially upon cooling for some solvents, for example, values of 15.5 for  $\text{CH}_2\text{Cl}_2$ <sup>[25,26]</sup> and 11.9 for THF<sup>[27,28]</sup> are recorded at 200 K, but not for others, for example, 2.47 at 240 K and 2.71 at 180 K for toluene.<sup>[26]</sup> On the other hand, these solvents have different coordinating and acid/base properties. THF is quite an efficient hydrogen-bond acceptor ( $E_j = 1.04$ ), better than  $\text{MeCN}$  ( $E_j = 0.75$ ),<sup>[29]</sup> although the latter is generally a better ligand for transition metals. Benzene and toluene are much weaker bases ( $E_j = 0.4$ ),<sup>[29]</sup> whereas  $\text{CH}_2\text{Cl}_2$  tends to behave more like a weak proton donor than as a proton acceptor.<sup>[24]</sup> We start by presenting the spectral features of the TFA proton donor in the  $\nu_{\text{CO}}$  region in various solvents, since the TFA/solvent interaction certainly plays an important role in the proton-transfer equilibria involving the hydride complex. The relevant spectra are shown in Figure 8. Two bands at similar frequencies are observed in  $\text{CH}_2\text{Cl}_2$

and toluene (1804 and 1785  $\text{cm}^{-1}$  for the former, 1803 and 1788  $\text{cm}^{-1}$  for the latter). The higher frequency band is due to the acid monomer, whereas the lower frequency one is typically assigned to the corresponding dimer.<sup>[30]</sup> Note that the equilibrium is shifted towards the dimer in toluene, as is evident from the different relative intensities. In THF the wide, asymmetric  $\nu_{\text{CO}}$  band of the acid monomer is greatly redshifted to 1780  $\text{cm}^{-1}$  because of the formation of stronger hydrogen bonds to solvent molecules. The shoulder at 1762  $\text{cm}^{-1}$  (which becomes a distinct band at 200 K) is assigned to the  $\text{CF}_3\text{COOH}$  dimer. The low-frequency asymmetry of the acid bands in all solvents suggests the presence of higher order TFA associates. Thus THF can form hydrogen bonds with  $\text{CF}_3\text{COOH}$ , lowering the activity of the acid, which is one of the reasons for the evolution of  $[\text{Cp}^*\text{Mo}(\text{dppe})\text{H}_4]^+\text{CF}_3\text{COO}^-$  into the final dihydride product in this solvent, as will be shown later.

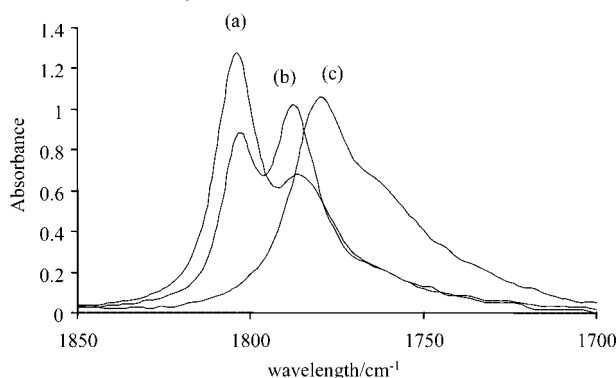


Figure 8. IR spectra of trifluoroacetic acid solutions (0.027 M, pathlength 0.04 mm) in various solvents at 290 K: (a)  $\text{CH}_2\text{Cl}_2$ ; (b) toluene; (c) THF.

### In Dichloromethane

Although the starting material and products are unstable in dichloromethane at room temperature, they do not decompose at low temperatures and this solvent has many advantages for infrared studies (it is not a strong proton acceptor, therefore it does not compete with the basic hydride complexes for hydrogen bonding, and it has good solvent properties for ionic compounds). An IR spectroscopic monitoring at 200 K in the acid  $\nu_{\text{CO}}$  and conjugated anion  $\nu_{\text{OCO}}^{\text{as}}$  vibration region yielded the results shown in Figure 9. At this temperature the dihydride complex  $[\text{Cp}^*\text{Mo}(\text{dppe})\text{H}_2(\text{O}_2\text{CCF}_3)]$ , which has a  $\nu_{\text{OCO}}^{\text{as}}$  at 1692  $\text{cm}^{-1}$  (vide infra), did not form.

A tentative assignment of all observed bands is possible on the basis of previous IR studies into the interaction between  $\text{CF}_3\text{COOH}$  and various bases,<sup>[30–32]</sup> in combination with the results shown in the previous section. At 200 K the acid self-association equilibrium is shifted to the dimer, exhibiting a strong band at 1780  $\text{cm}^{-1}$  with a shoulder at 1800  $\text{cm}^{-1}$  (Figure 9, b). The spectrum recorded for the solution with a  $\text{MoH}_3/\text{TFA}$  ratio of 1:0.5 (Figure 9, c) shows a prominent band at 1686  $\text{cm}^{-1}$  due to the  $\nu_{\text{OCO}}^{\text{as}}$  vibration of the trifluoroacetate anion. Its relatively sharp nature and almost negligible high frequency shift relative to

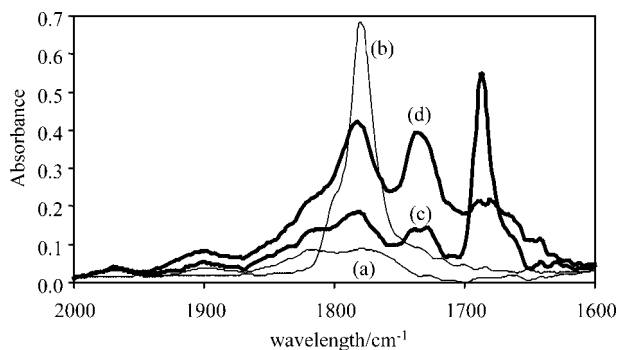
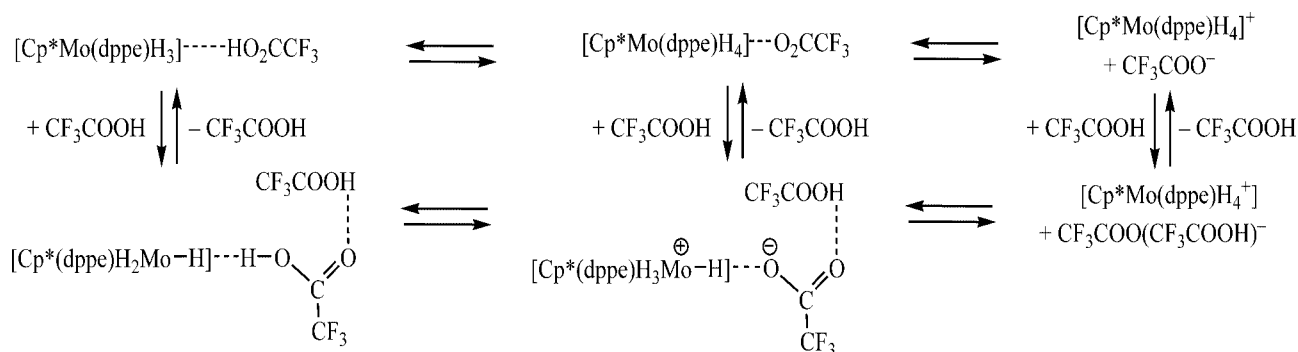


Figure 9. Low-temperature (200 K) IR spectra for the reaction between  $[\text{Cp}^*\text{Mo}(\text{dppe})\text{H}_3]$  and TFA in  $\text{CH}_2\text{Cl}_2$ : (a)  $[\text{Cp}^*\text{Mo}(\text{dppe})\text{H}_3]$  (0.028 M); (b) TFA (0.014 M); (c) mixture of  $[\text{Cp}^*\text{Mo}(\text{dppe})\text{H}_3]$  (0.028 M) and TFA (0.014 M); (d) mixture of  $[\text{Cp}^*\text{Mo}(\text{dppe})\text{H}_3]$  (0.028 M) and TFA (0.028 M).

the position of the free  $\text{CF}_3\text{COO}^-$  anion<sup>[31,32]</sup> indicates the formation of either a weakly H-bonded contact ion pair or a solvent-separated ion pair, consistent with the relatively high polarity of  $\text{CH}_2\text{Cl}_2$  at low temperatures and the poor proton-donor ability of the  $[\text{Cp}^*\text{Mo}(\text{dppe})\text{H}_4]^+$  cation. In reference to Scheme 1, this means that species V is extensively dissociated to VI or that the interaction is loose under these solvent and temperature conditions. There is no significant intensity in the region characteristic for the free homoconjugate anion,  $[\text{CF}_3\text{COO}(\text{CF}_3\text{COOH})_n]^-$ . According to the literature, this species should display a low intensity, broad band with a maximum at 1630–1620  $\text{cm}^{-1}$ .<sup>[33]</sup> Given the presence of an excess of the trihydride complex, most of the acid is presumably consumed and little is left to yield the homoconjugate anion. The relative intensity of the 1686  $\text{cm}^{-1}$  band indicates that the proton-transfer equilibrium is highly shifted to the tetrahydride product, and the presence of the unreacted trihydride complex is indicated by the shoulder at 1816  $\text{cm}^{-1}$  {cf. the starting spectrum of free  $[\text{Cp}^*\text{Mo}(\text{dppe})\text{H}_3]$  in Figure 9, a}. There are two additional weak bands in this spectrum. The first one at 1782  $\text{cm}^{-1}$  could be assigned to free  $\text{CH}_3\text{COOH}$ , but it is also consistent with a H-bonded adduct where the acid acts as a proton donor (a  $\text{CF}_3\text{COO}-\text{H}\cdots\text{B}$  interaction does not significantly perturb the CO normal mode). The second band at 1736  $\text{cm}^{-1}$  indicates the presence of a H-bonded adduct where the acid acts as a proton acceptor [the  $\text{CF}_3\text{C}(\text{OH})\text{O}\cdots\text{HA}$  interaction significantly redshifts the CO normal mode].<sup>[34,35]</sup> Thus, these bands constitute evidence for the presence of a 2:1 H-bonded adduct,  $[\text{Cp}^*\text{Mo}(\text{dppe})\text{H}_3]\cdots\text{HO}_2\text{CCF}_3\cdots\text{HO}_2\text{CCF}_3$ . The simultaneous presence of a 1:1 adduct,  $[\text{Cp}^*\text{Mo}(\text{dppe})\text{H}_3]\cdots\text{HO}_2\text{CCF}_3$ , cannot be established because it would also afford a band at ca. 1780  $\text{cm}^{-1}$ . A general picture of the proton-transfer process can be drawn as shown in Scheme 4.

An increase in the  $\text{CF}_3\text{COOH}/\text{MoH}_3$  ratio is expected to shift the hydrogen-bonding equilibrium position towards the 2:1 adduct. At the same time, equilibria involving the anionic species (either hydrogen bonded or free) are expected to shift towards the homoconjugate anion (equilibria



Scheme 4.

drawn vertically in Scheme 4). On the other hand, an increase in the  $\text{CF}_3\text{COOH}/\text{MoH}_3$  ratio will not affect the equilibria shown horizontally in Scheme 4. Indeed, upon addition of a second 0.5 equiv. TFA (final  $\text{MoH}_3/\text{TFA}$  ratio of 1:1), see Figure 9d, the IR spectrum reveals a significant increase in intensity for the bands assigned to the neutral 2:1 adduct and a dramatic decrease for that assigned to the free anion. The growth of a broad shoulder at lower frequencies signals the formation of anionic aggregates, as expected.

### In $[\text{D}_8]$ Toluene

The low-temperature IR spectral picture in  $[\text{D}_8]$ toluene in the presence of a stoichiometric amount of TFA is similar to that shown in dichloromethane, see Figure 10. The band at  $1742\text{ cm}^{-1}$  observed for the 1:1 mixture (Figure 10c) is assigned to the  $\nu_{\text{CO}}$  of the hydrogen-bonded complex (cf.  $1736\text{ cm}^{-1}$  in  $\text{CH}_2\text{Cl}_2$ ), whereas the bands at  $1690$  and  $1674\text{ cm}^{-1}$  are assigned to the  $\text{CF}_3\text{COO}^-$  anion ( $\nu_{\text{OCO}}^{\text{as}}$ , cf.  $1686\text{ cm}^{-1}$  in  $\text{CH}_2\text{Cl}_2$ ). The complex pattern attained for this absorption is possibly related to the presence of different hydrogen-bonded species (hydrogen bonding should be favored more in low-polarity toluene). The anion band did not show a significant increase in intensity at greater  $\text{MoH}_3/\text{TFA}$  ratios (1:0.5 or 1:0.2), indicating that the proton-transfer equilibrium is shifted further towards the neutral hydrogen-bonded species in this solvent in comparison with  $\text{CH}_2\text{Cl}_2$ . This agrees with the results of the NMR investigation. Upon warming above  $270\text{ K}$ , the bands corresponding to the  $[\text{Cp}^*\text{Mo}(\text{dppe})\text{H}_2(\text{O}_2\text{CCF}_3)]$  product at  $1702$  and  $1690\text{ cm}^{-1}$  quickly grow, while the shoulder at  $1674\text{ cm}^{-1}$  disappears. The final spectrum is shown in part d of Figure 10. Monitoring the growth of this band for the 1:1 reaction in  $\text{C}_6\text{H}_6$  at  $298\text{ K}$  (see Figure S3 in the Supporting Information) yielded a first-order rate constant of  $(1.8 \pm 0.1) \times 10^{-3}\text{ s}^{-1}$ . In the presence of a 3–5-fold excess of acid, the broad, low intensity  $\nu_{\text{OCO}}^{\text{as}}$  band of the homoconjugated anion was observed at ca.  $1640\text{ cm}^{-1}$ . No formation of  $[\text{Cp}^*\text{Mo}(\text{dppe})\text{H}_2(\text{O}_2\text{CCF}_3)]$  was observed under these conditions, in agreement with the NMR spectroscopic data.

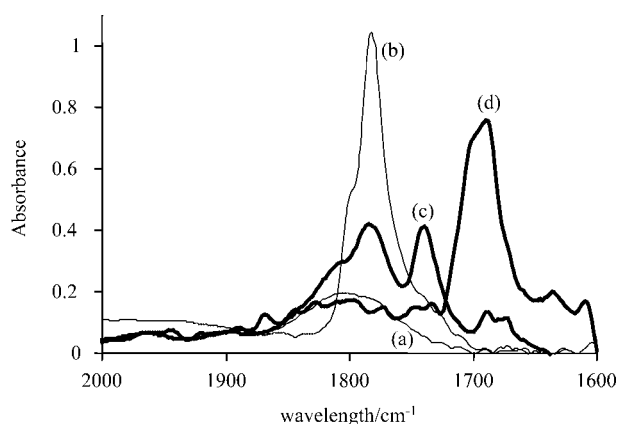


Figure 10. IR spectra for the reaction between  $[\text{Cp}^*\text{Mo}(\text{dppe})\text{H}_3]$  and TFA in  $[\text{D}_8]$ toluene: (a)  $[\text{Cp}^*\text{Mo}(\text{dppe})\text{H}_3]$  ( $0.027\text{ M}$ ) at  $200\text{ K}$ ; (b) TFA ( $0.027\text{ M}$ ) at  $200\text{ K}$ ; (c) 1:1 mixture ( $0.027\text{ M}$ ) at  $200\text{ K}$ ; (d) same mixture as (c), after complete conversion at room temperature.

### In THF

At low temperature in this solvent and in the presence of 1 equiv. TFA, the dominant species were the neutral hydrogen-bonded complexes, as indicated by the major bands at  $1784$  and  $1744\text{ cm}^{-1}$  (see Figure 11, c). No significant amounts of the  $\text{CF}_3\text{COO}^-$  ion were seen. This implies that proton transfer occurs to a smaller degree than in toluene. No homoconjugated anion band was observed upon raising the TFA excess to 5 equiv., in contrast to the results in aromatic hydrocarbon solution. Upon warming, the spectral changes were similar to those observed in toluene (see previous section), yielding  $[\text{Cp}^*\text{Mo}(\text{dppe})\text{H}_2(\text{O}_2\text{CCF}_3)]$ , see Figure 11 (d). We also investigated the reverse proton-transfer reaction by mixing together  $[\text{Cp}^*\text{Mo}(\text{dppe})\text{H}_4]^+\text{BF}_4^-$  {generated in situ at  $200\text{ K}$  from  $[\text{Cp}^*\text{Mo}(\text{dppe})\text{H}_3]$  and  $\text{HBF}_4$ } and  $\text{CF}_3\text{COONa}$  at  $200\text{ K}$  in THF. This experiment confirms the reversible nature of the proton-transfer process and the position of equilibrium. The essentially complete disappearance of the trifluoroacetate anion  $\nu_{\text{OCO}}^{\text{as}}$  bands at  $1702$  and  $1690\text{ cm}^{-1}$  and the growth of the  $\nu_{\text{CO}}$  band at  $1752\text{ cm}^{-1}$  corresponding to the H-bonded adduct<sup>[36]</sup> were observed at  $200\text{ K}$  in the presence of either 1

or 2 equiv.  $[\text{Cp}^*\text{Mo}(\text{dppe})\text{H}_4]^+\text{BF}_4^-$ . Subsequent warming to 290 K led once again to  $[\text{Cp}^*\text{Mo}(\text{dppe})\text{H}_2(\text{O}_2\text{CCF}_3)]$  formation.

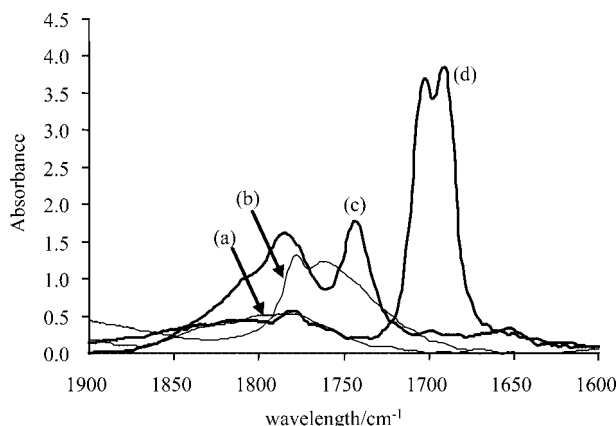


Figure 11. Low-temperature (200 K) IR spectra for the reaction of  $[\text{Cp}^*\text{Mo}(\text{dppe})\text{H}_3]$  with TFA in THF: (a)  $[\text{Cp}^*\text{Mo}(\text{dppe})\text{H}_3]$  (0.07 M); (b) TFA (0.07 M); (c) 1:1 mixture (0.07 M) at 200 K; (d) same mixture as (c), after complete conversion at room temperature.

Since the NMR-spectroscopic study shows that this conversion also occurs in the presence of excess acid, a kinetics investigation was carried out at 298 K using different TFA/Mo ratios. The reaction was found to be zero order with respect to the acid (see Table 3). Interestingly, the rate constant in THF is identical to that measured in benzene (vide supra) within experimental error. The study was also extended to different temperatures (using a TFA/Mo ratio of 1:1), with the subsequent Eyring analysis (see Supporting

Information) giving the following activation parameters:  $\Delta H^\ddagger = (31.8 \pm 0.5) \text{ kcal mol}^{-1}$  and  $\Delta S^\ddagger = (36 \pm 2) \text{ e.u.}$  The large positive activation entropy suggests that the transition state is dissociative in nature. At low temperatures, the rearrangement becomes too slow; for instance, reaction rate constants of  $5.2 \times 10^{-8}$  and  $5.8 \times 10^{-15} \text{ s}^{-1}$  are calculated at 250 and 200 K, respectively.

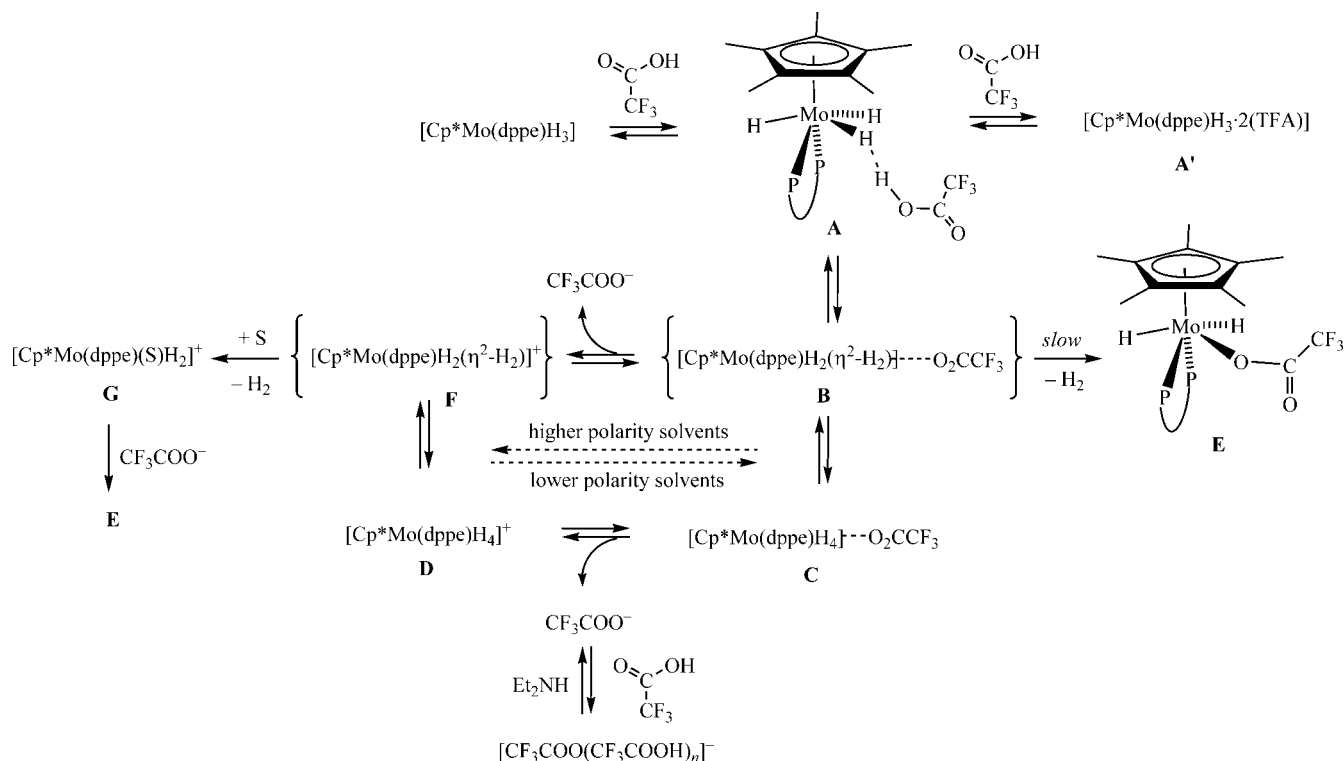
Table 3. Rate constants for the  $[\text{Cp}^*\text{Mo}(\text{dppe})\text{H}_2(\text{O}_2\text{CCF}_3)]$  formation reaction in THF;  $[\text{MoH}_3] = 0.025 \text{ M}$ .

$T/\text{K}$	TFA/Mo	$k/10^{-3} \text{ s}^{-1}$
280	1	$0.064 \pm 0.0015$
290	1	$0.63 \pm 0.01$
298	0.5	$1.7 \pm 0.1$
298	1	$1.8 \pm 0.1$
298	3	$1.9 \pm 0.1$
298	5	$1.80 \pm 0.05$
308	1	$13.7 \pm 0.2$

## Discussion

The collective observations that will be detailed now are summarized in Scheme 5.

Proton transfer to  $[\text{Cp}^*\text{Mo}(\text{dppe})\text{H}_3]$ , via the H-bonded adduct **A** to yield the classical tetrahydride complex,  $[\text{Cp}^*\text{Mo}(\text{dppe})\text{H}_4]^+$ , **C/D**, is the only reaction that may occur at low temperatures. The formation of the 2:1 H-bonded adduct **A'** was also evidenced by low-temperature IR spectroscopy, but one molecule of TFA is sufficient for proton transfer to occur, as also indicated by previous ki-



Scheme 5.

netics studies.<sup>[13]</sup> The proton transfer probably proceeds via a nonclassical intermediate (species **B** in Scheme 5), although we have not found any direct experimental evidence to support this proposition. Our recently reported theoretical calculations<sup>[13]</sup> indicate that the nonclassical complex lies in a very shallow minimum with a low barrier for conversion to the classical tetrahydride product, with the isomerization taking place without counteranion dissociation. The competitive dihydrogen evolution yielding  $[\text{Cp}^*\text{Mo}(\text{dppe})\text{H}_2(\text{O}_2\text{CCF}_3)]$  occurs only above 250 K and is possible (in noncoordinating solvents) by the reverse reaction between **D** and  $\text{CF}_3\text{COO}^-$ . This forms the ion pair **C** which subsequently isomerizes to the nonclassical species **B**.

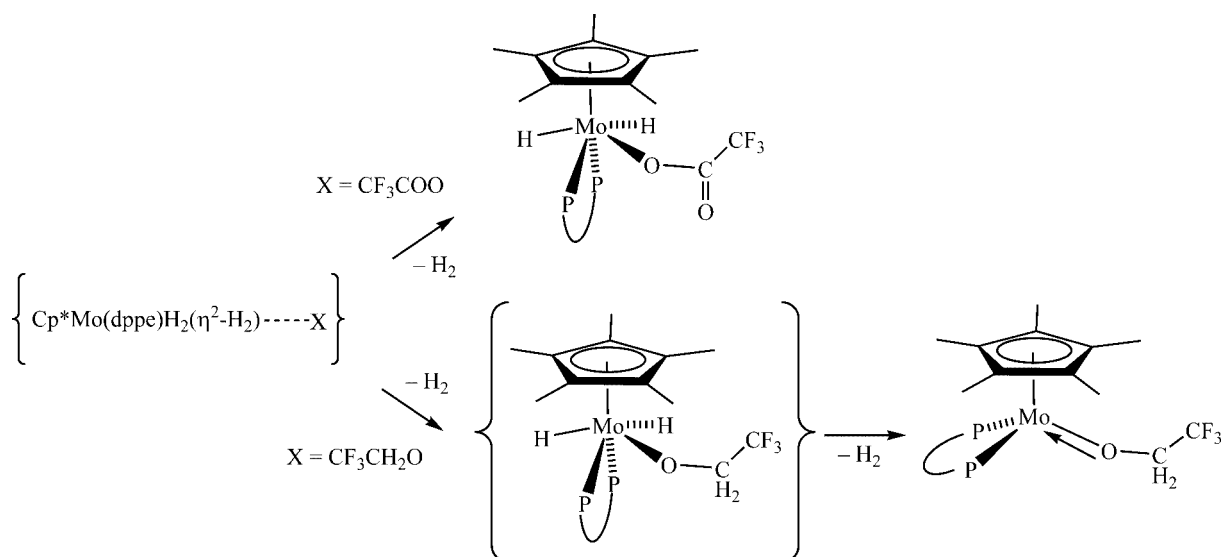
The formation of  $[\text{Cp}^*\text{Mo}(\text{dppe})\text{H}_4]^+$  is reversible below 250 K in contrast to the irreversible formation of *trans*- $\text{Cp}^*\text{MH}_2(\text{dppe})^+$  ( $\text{M} = \text{Fe}, \text{Ru}$ ).<sup>[6,8]</sup> One important difference between these systems is the reversibility of the nonclassical/classical isomerization for  $[\text{Cp}^*\text{Mo}(\text{dppe})\text{H}_4]^+$  (according to the DFT calculations), whereas this process is irreversible for  $[\text{Cp}^*\text{M}(\text{dppe})\text{H}_2]^+$  ( $\text{M} = \text{Fe}, \text{Ru}$ ). However, proton transfer to the hydride ligand is less thermodynamically favorable for  $[\text{Cp}^*\text{Mo}(\text{dppe})\text{H}_3]$  than for  $[\text{Cp}^*\text{Fe}(\text{dppe})\text{H}]$ ; a significant amount of TFA remained unreacted (in the H-bonded form) for a TFA/Mo ratio of 0.5 in  $\text{CH}_2\text{Cl}_2$  at 200 K (see Figure 9), whereas it was completely consumed under the same solvent, temperature, and stoichiometry conditions in the presence of  $[\text{Cp}^*\text{Fe}(\text{dppe})\text{H}]$ .<sup>[5]</sup> These results contrast with the higher basicity factor of  $[\text{Cp}^*\text{Mo}(\text{dppe})\text{H}_3]$  ( $E_j = 1.42 \pm 0.02$ )<sup>[13]</sup> relative to  $[\text{Cp}^*\text{Fe}(\text{dppe})\text{H}]$  ( $E_j = 1.36 \pm 0.02$ ).<sup>[7]</sup> The corresponding proton transfer to  $[\text{Cp}^*\text{Ru}(\text{dppe})\text{H}]$  ( $E_j = 1.39$ ), however, is also an equilibrium process.<sup>[6]</sup> The basicity factor correlates with the strength of the hydrogen bond (formation enthalpy), whereas the protonation equilibrium is determined by the free energy of the proton-transfer process. Obviously, the two parameters do not necessarily correlate quantitatively.

Both the  $\text{A} \rightleftharpoons \text{C/D}$  equilibrium position and rate of the irreversible  $[\text{Cp}^*\text{Mo}(\text{dppe})\text{H}_2(\text{O}_2\text{CCF}_3)]$  formation depend on the temperature, the solvent, and the  $\text{MoH}_3/\text{TFA}$  ratio. Polar solvents (e.g., dichloromethane at low temperatures, acetonitrile) weaken the hydrogen bond in **C** and lead to the formation of a solvent-separated ion pair (species **D** in Scheme 5), which stabilizes the tetrahydrido complex against the  $\text{H}_2$  loss. The proton-transfer equilibrium is shifted to species **D** in  $\text{CH}_2\text{Cl}_2$  even in the presence of stoichiometric amounts of the acid. Low-polarity solvents (e.g., toluene) provide less stabilization for the charged species, thus the proton-transfer equilibrium is shifted to the left when near stoichiometric amounts of the acid are used. The tetrahydride product exists as an ion pair stabilized by hydrogen bonding to the  $\text{CF}_3\text{COO}^-$  anion (species **C** in Scheme 5), as reflected for instance in a reduced rate of hydride site exchange measured by  $^1\text{H}$  NMR spectroscopy below 240 K. The formation of hydrogen-bonded ion pairs of 1:1 composition was also confirmed for weaker proton donors.<sup>[13]</sup> At room temperature and above, the competitive irreversible  $\text{H}_2$  elimination process eventually leads to the

quantitative formation of the final product **E**. However, excess acid favors ion-pair dissociation through formation of the thermodynamically more stable homoconjugate anion, thereby stabilizing the proton-transfer product **D** and precluding the  $\text{H}_2$  evolution.

In solvents with proton-accepting ability (THF, MeCN) the activity of the acid is reduced by hydrogen bonding with solvent molecules, formation of the homoconjugated anion is not observed, and the reaction yields **E** even in the presence of excess acid. The attainment of the same formation rate constant in THF and in benzene and the zero-order dependence on TFA agree with the proposed unimolecular generation of **E** from the same intermediate **B**. Furthermore, the large positive activation entropy is consistent with a dissociative mechanism (i.e.,  $\text{H}_2$  must leave before the trifluoroacetate anion can coordinate), as may be expected from the electronically saturated nature of system **B**. The rate of formation in MeCN was not determined with accuracy, but the NMR spectroscopic data in Figure 7 allow us to estimate a rate constant of ca.  $2 \times 10^{-3} \text{ s}^{-1}$ , that is, close to that determined in THF and benzene (see Table 3), if we assume a first-order decay process is in operation. The high polarity of MeCN favors proton transfer and ion-pair dissociation through the stabilization of the charge-separated species, but the instability of  $[\text{Cp}^*\text{Mo}(\text{dppe})\text{H}_4]^+$  leads to its ultimate decomposition by  $\text{H}_2$  elimination. In this case, the process may be solvent-assisted, leading to the solvent adduct **G**, as previously established by the protonation with  $\text{HBF}_4$ .<sup>[14]</sup> This phenomenon also occurs in THF as verified by using  $\text{HBF}_4$ . However, the  $\text{CF}_3\text{COO}^-$  anion has a stronger coordinating power than both THF and MeCN, and the ultimate product is once again **E**.

Species **A** and **C/D** exhibit a dynamic exchange process, as revealed by a broad  $^1\text{H}$  resonance at room temperature which decoalesces at 270 K in  $\text{C}_6\text{D}_5\text{CD}_3$  for the mixture containing 1 equiv. TFA. This results from the fast and direct unimolecular proton transfer involving the dihydrogen-bonded complex **A** and the H-bonded ion pair **C**. It is not possible, unfortunately, to use this information to derive an accurate value for the proton-transfer rate constant because of the complexity of the coupled equilibria and the irreversible transformation to product **E**. Assuming, however, that only species **A** and **C** are present in an approximately equimolar ratio, an activation barrier  $\Delta G^\ddagger$  of  $11.7 \text{ kcal mol}^{-1}$  may be estimated for the proton transfer in  $\text{C}_6\text{D}_5\text{CD}_3$  at 270 K, from the coalescence temperature and the chemical shift difference.<sup>[37]</sup> This activation barrier is lower than that of the proton transfer by HFIP in toluene ( $\Delta G_{293 \text{ K}}^\ddagger = 15.8 \text{ kcal mol}^{-1}$ ),<sup>[13]</sup> in agreement with the higher proton-donating ability of TFA. It is also lower than  $\Delta G_{270 \text{ K}}^\ddagger$  for the proton transfer from HFIP to  $[\text{Cp}^*\text{Fe}(\text{dppe})\text{H}]$  in  $\text{CH}_2\text{Cl}_2$  ( $14.7 \text{ kcal mol}^{-1}$ ) or from PFTB to  $[\text{CpRuH}(\text{CO})(\text{PCy}_3)]$  in hexane ( $16.1 \text{ kcal mol}^{-1}$ ), calculated for 270 K using the published activation parameters.<sup>[3,5]</sup> IR kinetic data (vide supra) give  $\Delta G_{270 \text{ K}}^\ddagger = 22.1 \text{ kcal mol}^{-1}$  for the dihydrido-trifluoroacetate formation. The irreversibility of the  $\text{H}_2$  evolution process renders  $[\text{Cp}^*\text{Mo}(\text{dppe})\text{H}_2(\text{O}_2\text{CCF}_3)]$  the sole end product.



Scheme 6.

A final point of interest is a comparison between the results shown here and those reported previously for the decomposition of the proton-transfer product obtained with TFE, which led to a diamagnetic hydride-free decomposition product,  $[\text{Cp}^*\text{Mo}(\text{dppe})(\text{OCH}_2\text{CF}_3)(\text{TFE})_x]$  ( $x = 0$  or  $1$ ). The mechanism is likely to be the same for both systems, leading to a first  $\text{H}_2$  elimination assisted by the coordination of the alkoxide ligand (see Scheme 6). Why does  $[\text{Cp}^*\text{Mo}(\text{dppe})\text{H}_2(\text{O}_2\text{CCF}_3)]$  show no tendency to expel a second  $\text{H}_2$  molecule and form the hypothetical compound  $[\text{Cp}^*\text{Mo}(\text{dppe})(\text{O}_2\text{CCF}_3)]$ , in which the trifluoroacetate ligand would bind in a chelating fashion, whereas  $[\text{Cp}^*\text{Mo}(\text{dppe})\text{H}_4]^+(\text{OCH}_2\text{CF}_3)$  leads to a hydride-free product without the observation of even trace amounts of a dihydride intermediate? A possible rationalization is that the stronger  $\pi$ -donating ability of the oxygen lone pairs in the fluorinated alkoxide ligand may assist the elimination of the second  $\text{H}_2$  molecule by stabilizing the resulting 16-electron half-sandwich  $\text{Mo}^{\text{II}}$  product. By contrast, the lone pair of the trifluoroacetate oxygen donor atom is not sufficiently basic and the second oxygen atom is presumably not capable of assisting the  $\text{H}_2$  elimination process, because of either thermodynamic or kinetic reasons.

## Conclusions

We explored the protonation of  $[\text{Cp}^*\text{Mo}(\text{dppe})\text{H}_3]$  by trifluoroacetic acid in various solvents which display different proton-accepting ability, polarity, and coordinating power toward transition metals: dichloromethane, benzene/toluene, THF, and MeCN. The nature of the solvent and the amount of excess acid determined the nature of the product by delicately controlling the position of the proton transfer and ion pairing equilibria. In agreement with previous investigations, the classical tetrahydrido cation was produced following the initial formation of a dihydrogen-bonded intermediate without the observation of a nonclassical tauto-

mer (dihydrogen complex); it is stable at low temperatures and can exist as solvent-separated or contact ion pair. However, the use of suitable conditions of solvent, temperature, and hydride/acid ratio led to the selective formation of a new product, the dihydrido complex  $[\text{Cp}^*\text{Mo}(\text{dppe})\text{H}_2(\text{O}_2\text{CCF}_3)]$ . The trifluoroacetate anion is a sufficiently strong ligand to coordinate to the cationic complex and saturate its coordination sphere after loss of  $\text{H}_2$ , even in the presence of coordinating solvent molecules such as MeCN or THF. However, it remains coordinated in a monodentate fashion and, contrary to the  $\text{CF}_3\text{CH}_2\text{O}^-$  anion, is not capable of inducing the elimination of the residual hydride ligands as  $\text{H}_2$  to form a hydride-free product.

## Experimental Section

**General:** All manipulations were performed under argon by standard Schlenk techniques. All solvents were dried with an appropriate drying agent (Na/benzophenone for benzene, toluene or THF; Na for pentane;  $\text{CaH}_2$  for  $\text{CH}_2\text{Cl}_2$ ) and were freshly distilled under argon prior to use.  $\text{C}_6\text{D}_6$ ,  $\text{C}_6\text{D}_5\text{CD}_3$ ,  $[\text{D}_8]\text{thf}$ ,  $\text{CD}_3\text{CN}$ , and  $\text{CD}_2\text{Cl}_2$  (Euriso-Top) for NMR spectroscopic experiments and  $\text{C}_6\text{D}_5\text{CD}_3$  (Aldrich) for IR spectroscopic experiments were degassed by three freeze-pump-thaw cycles, and then purified by vacuum transfer at room temp.  $[\text{Cp}^*\text{Mo}(\text{dppe})\text{H}_3]$  was synthesized according to the literature.<sup>[14]</sup>

### Spectroscopic Studies

**NMR Investigations:** Samples of  $[\text{Cp}^*\text{Mo}(\text{dppe})\text{H}_3]$  in each solvent were prepared under argon in 5-mm NMR tubes. The  $^1\text{H}$ - and  $^{31}\text{P}\{^1\text{H}\}$  NMR data were collected with Bruker AMX300 and Bruker AV500 spectrometers, operating at 300.1 or 500.3 MHz and 121.5 or 202.5 MHz, respectively. The temperature was calibrated using a methanol chemical-shift thermometer; the accuracy and stability was  $\pm 1$  K. All samples were allowed to equilibrate at every temperature for at least 3 min. The spectra were calibrated with the residual solvent resonance ( $^1\text{H}$ ) and with external 85%  $\text{H}_3\text{PO}_4$  ( $^{31}\text{P}$ ). The conventional inversion-recovery method ( $180-\tau-90$ ) was

used to determine the variable-temperature longitudinal relaxation time  $T_1$ . Standard Bruker software was used for the calculation of the longitudinal relaxation time.

**IR-Spectroscopic Investigations:** The IR measurements were performed with the "Infracum 801" FTIR spectrometer using CaF<sub>2</sub> cells of 0.04-cm path length. All IR measurements were carried out by the use of a home-modified cryostat (Carl Zeiss Jena) in the 190–290 K temperature range. The cryostat modification allowed operation under an inert atmosphere and the transfer of the reagents (premixed either at low or room temp.) directly into the cell precooled to the required temperature. The accuracy of the temperature adjustment was  $\pm 1$  K. This setup was used both for the variable-temperature studies and for the kinetics investigations.

**Synthesis of [Cp\*Mo(dppe)H<sub>2</sub>(O<sub>2</sub>CCF<sub>3</sub>):** A CF<sub>3</sub>COOH solution (9.5  $\mu$ L, 0.13 mmol) in THF (3 mL) was slowly added to a solution of [Cp\*Mo(dppe)H<sub>3</sub>] (80 mg, 0.13 mmol) in THF (15 mL). The reaction mixture was stirred at room temp. for ca. 1.5 h. The solvent was evaporated, and the resulting solid was recrystallized from pentane. Yield: 75 mg (78%). <sup>1</sup>H NMR (300.13 MHz, C<sub>6</sub>D<sub>6</sub>, 290 K):  $\delta$  = -5.09 (Mo–H<sub>2</sub>), 1.79 (s, 15 H, Cp\*), 3.2–2.5 (m, 4 H, –CH<sub>2</sub>–CH<sub>2</sub>–), 7.10–7.77 (m, 20 H, Ph) ppm. <sup>31</sup>P{<sup>1</sup>H} NMR (121.5 MHz, C<sub>6</sub>D<sub>6</sub>, 290 K):  $\delta$  = 76.9 (s) ppm. The <sup>1</sup>H hydride and the <sup>31</sup>P resonances decoalesce at low temperatures (see Results section). IR (KBr):  $\tilde{\nu}$  = 1682 and 1702 (sh) (v<sup>as</sup><sub>OCO</sub>), 1818 and 1850 (Mo–H<sub>2</sub>) cm<sup>-1</sup>. C<sub>38</sub>H<sub>41</sub>F<sub>3</sub>MoO<sub>2</sub>P<sub>2</sub> (744.6): calcd. C 61.29, H 5.56; found C 61.26, H 5.54. Crystals were grown by slow diffusion of a pentane layer into a saturated solution of the mixture containing [Cp\*Mo(dppe)H<sub>3</sub>] and ca. 1 equiv. of TFA in toluene.

**Kinetics of the [Cp\*Mo(dppe)H<sub>2</sub>(O<sub>2</sub>CCF<sub>3</sub>) Formation:** The reagents were mixed at low temperature (ca. 270 K), and the solution was transferred into the cryostat. The kinetics data were obtained by following the increase of the band at 1692 cm<sup>-1</sup> corresponding to the [Cp\*Mo(dppe)H<sub>2</sub>(O<sub>2</sub>CCF<sub>3</sub>)] complex at the desired temperature. The first-order rates were obtained by plotting  $\ln(A_\infty - A_t)$  versus time  $t$ .

**X-ray Analysis of Compound [Cp\*Mo(dppe)H<sub>2</sub>(O<sub>2</sub>CCF<sub>3</sub>):** A single crystal was mounted under inert perfluoropolyether on the tip of a glass fiber and cooled in the cryostream of the Oxford-Diffraction XCALIBUR CCD diffractometer. Data were collected using the monochromatic Mo-K $\alpha$  radiation ( $\lambda$  = 0.71073). The structure was solved by direct methods (SIR97)<sup>[38]</sup> and refined by least-squares procedures on  $F^2$  using SHELXL-97.<sup>[39]</sup> All hydrogen atoms attached to carbon were introduced in the calculation in idealized positions and treated as riding models. The two hydride ligands were located in difference Fourier syntheses, and they were freely refined with isotropic thermal parameters. The molecule was drawn with the help of ORTEP32.<sup>[40]</sup> Crystal data and refinement parameters are shown in Table 4.

CCDC-632317 contains the supplementary crystallographic data for this paper. These data can be obtained free of charge from The Cambridge Crystallographic Data Centre via www.ccdc.cam.ac.uk/data\_request/cif.

**Supporting Information** (see also the footnote on the first page of this article): Table of longitudinal relaxation times at different temperatures for the hydride resonance of [Cp\*Mo(dppe)H<sub>2</sub>(O<sub>2</sub>CCF<sub>3</sub>)] and figures showing IR spectra of this compound in various solvents, the IR-spectroscopic study of its formation kinetics in toluene, and an Eyring plot of the rate constants in THF.

Table 4. Crystal data and structure refinement for compound [Cp\*Mo(dppe)H<sub>2</sub>(O<sub>2</sub>CCF<sub>3</sub>)].

Empirical formula	C <sub>38</sub> H <sub>41</sub> F <sub>3</sub> MoO <sub>2</sub> P <sub>2</sub>	
Formula weight	744.59	
Temperature	180(2) K	
Wavelength	0.71073 Å	
Crystal system	monoclinic	
Space group	P2 <sub>1</sub> /n	
Unit cell dimensions	$a = 11.2103(4)$ Å	$a = 90^\circ$
	$b = 15.0429(7)$ Å	$\beta = 93.675(3)^\circ$
	$c = 20.1563(7)$ Å	$\gamma = 90^\circ$
Volume	3392.1(2) Å <sup>3</sup>	
Z	4	
Density (calculated)	1.458 Mg m <sup>-3</sup>	
Absorption coefficient	0.531 mm <sup>-1</sup>	
$F(000)$	1536	
Crystal size	0.57 × 0.3 × 0.28 mm	
Theta range for data collection	2.96–30.03°	
Index ranges	-15 ≤ $h$ ≤ 15, -12 ≤ $k$ ≤ 21, -28 ≤ $l$ ≤ 28	
Reflections collected	31116	
Independent reflections	9836 [ $R_{\text{int}} = 0.0477$ ]	
Completeness to $\theta = 30.00^\circ$	99.1%	
Absorption correction	semi-empirical from equivalents	
Max. / min. transmission	0.9726 / 0.7281	
Refinement method	full-matrix least-squares on $F^2$	
Data / restraints / parameters	9836 / 0 / 428	
Goodness-of-fit on $F^2$	1.082	
Final $R$ indices [ $I > 2\sigma(I)$ ]	$R_1 = 0.0403$ , $wR_2 = 0.1022$	
$R$ indices (all data)	$R_1 = 0.0480$ , $wR_2 = 0.1072$	
Largest diff. peak and hole	1.193 and -1.187 e Å <sup>-3</sup>	

## Acknowledgments

We thank the European Commission, HYDROCHEM program (contract HPRN-CT-2002-00176) for support of this work. Additional support from the Centre National de la Recherche Scientifique (CNRS, program PICS), France, from the Russian Foundation for Basic Research (RFBR) (05-03-22001, 05-03-32415) and the Division of Chemistry and Material Sciences of RAS, Russia, is also gratefully acknowledged. N. V. B. thanks Russian Science Support Foundation for an individual grant. M. B. thanks the Ministerio de Educación y Ciencia (MEC) for a post-doctoral fellowship.

- [1] N. V. Belkova, E. S. Shubina, L. M. Epstein, *Acc. Chem. Res.* **2005**, *38*, 624.
- [2] N. V. Belkova, A. V. Ionidis, L. M. Epstein, E. S. Shubina, S. Gruendemann, N. S. Golubev, H. H. Limbach, *Eur. J. Inorg. Chem.* **2001**, 1753.
- [3] N. Belkova, M. Besora, L. Epstein, A. Lledós, F. Maseras, E. Shubina, *J. Am. Chem. Soc.* **2003**, *125*, 7715.
- [4] E. Gutsul, N. Belkova, G. Babakhina, L. Epstein, E. Shubina, C. Bianchini, M. Peruzzini, F. Zanobini, *Russ. Chem. Bull.* **2003**, *52*, 1204.
- [5] N. V. Belkova, E. Collange, P. Dub, L. M. Epstein, D. A. Lemenovskii, A. Lledós, O. Maresca, F. Maseras, R. Poli, P. O. Revin, E. S. Shubina, E. V. Vorontsov, *Chem. Eur. J.* **2005**, *11*, 873.
- [6] N. V. Belkova, P. A. Dub, M. Baya, J. Houghton, *Inorg. Chim. Acta* **2007**, *360*, 149.
- [7] N. V. Belkova, P. O. Revin, L. M. Epstein, E. V. Vorontsov, V. I. Bakhmutov, E. S. Shubina, E. Collange, R. Poli, *J. Am. Chem. Soc.* **2003**, *125*, 11106.
- [8] M. Baya, O. Maresca, R. Poli, Y. Coppel, F. Maseras, A. Lledós, N. V. Belkova, P. A. Dub, L. M. Epstein, E. S. Shubina, *Inorg. Chem.* **2006**, *45*, 10248.

- [9] M. S. Chinn, D. M. Heinekey, *J. Am. Chem. Soc.* **1990**, *112*, 5166.
- [10] E. S. Shubina, N. V. Belkova, E. V. Bakhmutova, E. V. Vorontsov, V. I. Bakhmutov, A. V. Ionidis, C. Bianchini, L. Marvelli, M. Peruzzini, L. M. Epstein, *Inorg. Chim. Acta* **1998**, *280*, 302.
- [11] N. V. Belkova, E. S. Shubina, E. I. Gutsul, L. M. Epstein, I. L. Eremenko, S. E. Nefedov, *J. Organomet. Chem.* **2000**, *610*, 58.
- [12] S. Gründeman, S. Ulrich, H.-H. Limbach, N. S. Golubev, G. S. Denisov, L. M. Epstein, S. Sabo-Etienne, B. Chaudret, *Inorg. Chem.* **1999**, *38*, 2550.
- [13] N. V. Belkova, P. O. Revin, M. Besora, M. Baya, L. M. Epstein, A. Lledós, R. Poli, E. S. Shubina, E. V. Vorontsov, *Eur. J. Inorg. Chem.* **2006**, 2192.
- [14] B. Pleune, R. Poli, J. C. Fettinger, *Organometallics* **1997**, *16*, 1581.
- [15] J. Andrieu, N. V. Belkova, M. Besora, E. Collange, L. M. Epstein, A. Lledós, R. Poli, P. O. Revin, E. S. Shubina, E. V. Vorontsov, *Russ. Chem. Bull.* **2003**, *52*, 2679.
- [16] J. H. Shin, D. G. Churchill, G. Parkin, *J. Organomet. Chem.* **2002**, *642*, 9.
- [17] E. Le Grogne, R. Poli, P. Richard, *Organometallics* **2000**, *19*, 3842.
- [18] M. A. A. F. D. C. T. Carrondo, M. J. Calhorda, M. B. Hursthouse, *Acta Crystallogr., Sect. C: Cryst. Struct. Commun.* **1987**, *43*, 880.
- [19] T. Steiner, *J. Chem. Crystallogr.* **1999**, *29*, 1235.
- [20] L. M. Epstein, L. N. Saitkulova, G. P. Zol'nikova, D. N. Kravtsov, *Metalloorganicheskaya Khimiya* **1991**, *4*, 1368.
- [21] The starting material contains a minor amount of the [Cp\*Mo( $\kappa^1$ -dppe)H<sub>3</sub>] contaminant, which is characterized by a doublet resonance at -3.09 ppm in the <sup>1</sup>H NMR spectrum and by a singlet at 57.2 ppm in the <sup>31</sup>P{<sup>1</sup>H} NMR spectrum. This is the typical by-product of the [Cp\*Mo(dppe)H<sub>3</sub>] synthesis<sup>[13]</sup> and is present in variable amounts in different samples. It is rather difficult to completely remove this impurity, but its presence does not interfere with the observed transformations since it is less basic than the trihydride complex (thus is not consumed when using substoichiometric amounts of TFA), whereas it is transformed into the trihydride complex with H<sub>2</sub> evolution by an excess amount of the acid.
- [22] These two resonances are sufficiently sharp for detection only on a high-field instrument (<sup>31</sup>P resonance at 202 MHz).
- [23] E. S. Shubina, N. V. Belkova, A. N. Krylov, E. V. Vorontsov, L. M. Epstein, D. G. Gusev, M. Niedermann, H. Berke, *J. Am. Chem. Soc.* **1996**, *118*, 1105.
- [24] C. Reichardt, *Solvents and Solvent Effects in Organic Chemistry*, 3rd ed., WILEY-VCH, Weinheim, **2003**.
- [25] S. O. Morgan, H. H. Lowry, *J. Phys. Chem.* **1930**, *34*, 2385.
- [26] S. Sharif, G. S. Denisov, M. D. Toney, H.-H. Limbach, *J. Am. Chem. Soc.* **2006**, *128*, 3375.
- [27] C. Carvajal, K. J. Tolle, J. Smid, M. Szwarc, *J. Am. Chem. Soc.* **1965**, *87*, 5548.
- [28] D. J. Metz, A. Glines, *J. Phys. Chem.* **1967**, *71*, 1158.
- [29] A. V. Iogansen, *Theor. Experim. Khim.* **1971**, *7*, 302.
- [30] J. Z. Dega-Szafran, M. Grundwald-Wyspianska, M. Szafran, *Spectrochim. Acta, Ser. A* **1991**, *47*, 543.
- [31] L. M. Epstein, A. N. Krylov, E. S. Shubina, *J. Mol. Struct.* **1994**, *322*, 345.
- [32] E. S. Shubina, A. N. Krylov, N. V. Belkova, L. M. Epstein, A. P. Borisov, V. D. Mahaev, *J. Organomet. Chem.* **1995**, *493*, 275.
- [33] W. Klemperer, G. C. Pimentel, *J. Chem. Phys.* **1954**, *22*, 1399.
- [34] J. P. Castaneda, G. S. Denisov, S. Y. Kucherov, V. M. Schreiber, A. V. Shurukhina, *J. Mol. Struct.* **2003**, *660*, 25.
- [35] G. V. Gusakova, G. S. Denisov, A. L. Smolyanskii, *Optika i Spektroskopiya* **1972**, *32*, 922.
- [36] This band is slightly shifted relative to that obtained upon the interaction of [Cp\*Mo(dppe)H<sub>3</sub>] with TFA, because of the effect of the Na<sup>+</sup> and BF<sub>4</sub><sup>-</sup> present in solution.
- [37] J. Sandström, *Dynamic NMR Spectroscopy*, Academic Press, London, **1982**.
- [38] A. Altomare, M. Burla, M. Camalli, G. Cascarano, C. Giacovazzo, A. Guagliardi, A. Moliterni, G. Polidori, R. Spagna, *J. Appl. Crystallogr.* **1999**, *32*, 115.
- [39] G. M. Sheldrick, *SHELXL97. Program for Crystal Structure Refinement*, University of Göttingen, Göttingen, Germany, **1997**.
- [40] L. J. Farrugia, *J. Appl. Crystallogr.* **1997**, *30*, 565.

Received: January 7, 2007  
Published Online: April 17, 2007